Response to Reviewers

Reviewer 1 (Favillier):

We appreciate the thorough review of our manuscript and the constructive feedback provided by Adrien Favillier. Here, we address each comment and reference the changes in the revised manuscript. We are pleased that the reviewer recommends this work be published in NHESS after the appropriate revisions are addressed. We've posted the responses below for timely discussion and will provide a complete revised manuscript after receiving comments from other reviewers and the editor.

Comment:
First of all, as a non-native speaker, some paragraphs, especially related to the numerous abbreviations (although necessary), remain complex and sometimes not fluent enough to clearly understand the developed idea at the first reading. Revising the manuscript with the aim to make it clearer and easy/fluent to read would be great, especially for non-native speakers.
Response:
We revised the writing to be more succinct and accessible throughout the manuscript.

Comment:
Second, there is a major mistake in the Wit formula (2) which partially distorts the results. At the difference of Kogelnig-Mayer et al. (2011), in the 4-Steps procedure developed by Favillier et al. (2017, 2018), the weighted sum of the first term is not multiplied by the total of growth disturbance of the year t. To use the Wit threshold initially defined in Favillier et al. (2017, 2018), please use the formula presented at the pages 93 and 14, respectively, of these articles. Otherwise, please define new thresholds that could represent your range of values. At the end, results should be nearly the same as you had the opportunities to work with many cross-sections.
Response:
Thanks for the careful attention to detail on this equation. Fortunately, this was simply a typo in the equation in the manuscript. We used the eqn. from Favillier et al. (2017, 2018) in the analysis, but accidentally inserted the R_t term from the Kogelnig-Mayer et al. (2011) eqn. in the manuscript. Equation (2) revised to reflect this.

Comment:
L.60-66: According to the table title, Table 1 appears incomplete (21 references over the 42 existing studies with more than one avalanche path). Precisely, what were your selection criteria? Please either clarify the caption or add the missing references.
Response:
We included only the initial studies using a dataset with more than one avalanche path. In other words, if a study used the same dataset again in subsequent work, then, instead of repeating this in the table, we omitted it. We revised the table caption to clarify this and also moved the table to Appendix A as Table A1 as per Reviewer 2.

Comment:
L.124-126 (Table 2): Please, modify "n" for "Trees (n)" or "Nb. of trees (n)" in order to be clearer that "n" is for the number of sampled trees per path.
Response:
2nd column in current Table 1 changed to "Trees (n)". Line 118.

Comment:
L.167: As you mainly worked with dead trees, how did you deal with? Did you take account of their year of death? Did you take account of the forest age structure of the path to suspect past high magnitude event that partially destroyed the forest?
Response:
Yes, we took into account the death year. We did not quantify or relate any death dates to avalanches that fell outside of observed avalanche mortality events. We assigned C-1 events to trees that were known to be killed by an avalanche impact, in-place trees with earlywood growth for the year of the observed avalanche event.

Comment:
L.197-204: This comparison makes sense in a general methodological point of view (how much growth disturbance are we missing using core instead of cross-section).
However, it does not match the main aims of the article and, accordingly, complexifie the reading. I suggest removing the comparison and the related paragraphs, but to discuss the advantages/limits to work with cross-sections in the Discussion section. On the one hand, knowing all the growth disturbances strengthen the reliability of your reconstructions. On the other hand, cross-sections are usually taken out from dead trees, so you cannot really assess the age structure of the in-place forest. Moreover, it is time consuming to process in comparison to cores, as you will have to carefully analyze the whole section. Lastly, it is an exceptional situation, as in Europe, we are mostly working on living trees in protection forest.
Response:
We believe that the results of this analysis in examining cores vs. cross-sections align with the objectives of the article. Determining the value of using cross-sections was central to the original sampling design which distinguishes this study from previous dendro-avalanche research. The exercise must be mentioned in the Methods section because we present values on the comparisons in the Results and then the Discussion. Lastly, we provide this comparison to simply quantitatively illustrate the difference in using cross sections vs. cores and do not in any way discount any studies that use cores.
Regarding the “age structure of the in-place forest”: we did not sample/process GDs to identify stand replacing large magnitude avalanche events using age structure cohort recruitment methods, similar to those used in fire or other ecological studies. The stems sampled from mixed subalpine forests were of great variation in ages. All the forests we worked in across the northern Rockies have mixed age structure due to varied disturbances, so quantifying a stand age structure is usually not possible, or all that informative relative to the growth disturbance information provided by cross-sections. Appropriately, we offer no unsubstantiated conjecture relating previous large magnitude events to the age structure of trees sampled in the paths. While it can be more time consuming to process cross-sections vs. cores, we utilized the opportunity to collect cross-sections for a more complete perspective and ability to identify GDs with greater confidence.
Regarding the last sentence in the comment: we were also constrained from sampling trees within a "protected forest" as a U.S. National Park prohibits wood collection on its lands except in the case of permitted research.

Comment:
L.299 (Fig. 3): In my opinion, the term "event" is not really suitable as it refers to crossdated growth disturbances and not to a reconstructed avalanche event. Responses, as mentioned in the figure title, could fit.
Response:
We changed the figure slightly in response to Reviewer 2’s comments. Therefore, the proportions are included in Figure 3(a). We also revised the X-axis title for panel (a) to “Classification of Each Response” to fit with the Y-axis title.

Comment:
L.327-328 (Fig. 5): The name of the Y-axis and the captions are not really clear. I suggest replacing "Avalanche path" by "Avalanche event."
Response:
The Y-axis title should read "...Avalanche Paths" as it currently stands. This figure highlights the number of avalanche paths in which an avalanche event occurred in any given year. We revised the figure caption to be clearer. Line 330.

Comment:
L.460 (Fig. 8): Graphs (a) and (c) could deserve a secondary axis for (a) the sample size and (c) the number of avalanche path. It would be easier to read. Here is the R-code I use to plot a secondary axis: ylim.prim <- c(0, max(Growth Disturbances, na.rm = T)) # Primary axis: distance to zero ylim.sec <- c(0, max(Sample Size, na.rm = T)) #Secondary axis: distance to zero b <- diff(ylim.prim)/diff(ylim.sec) #Computing multiplicative coefficient a <- b*(ylim.prim[1] - ylim.sec[1]) #Distance to zero ggplot(data, aes(x=Years))+ geom_line(aes(y = Growth Disturbances))+ #Primary axis geom_line(mapping = aes(y = a+Sample Size*b))+ #Secondary axis scale_y_continuous(sec.axis = sec_axis(_ (. - a)/b, name = "Sample Size"))
Response:
First, thank you very much for the R-code. We greatly appreciate it. We contemplated, at length, adding a secondary axis for these exact plots prior to submission. We typically use one primary axis for ease of interpretation for the reader. However, in this case we feel the secondary axis might be appropriate. As such we revised the figure and explicitly note the secondary axis for panels (a) and (c) in the new caption for Figure 8.

Comment:
L.432–433: What is the purpose of this comparison? I suggest removing it to simplify the manuscript.
Response:
We removed this sentence as it did not fit within the context of this paragraph.

Comment:
TECHNICAL COMMENTS Please, carefully revise the manuscript to tackle the typos. Most of them are located in the figure references in the text (extra brackets).
Response:
We corrected the typos throughout the manuscript.

Reviewer 2 (Luckman):

We appreciate the thorough review of our manuscript and the constructive feedback provided by Brian Luckman. Here, we address each comment and reference the changes in the revised manuscript.

Comment:
The use of symbols to identify important terms is difficult to follow e.g Wit, RAAIt etc and a table describing these terms (in words) would be a useful addition. One of the principal difficulties is the comparison of statistics such as RI values between sites based on records of different length where the RI values are strongly related to survival of older individuals within the avalanche path. Perhaps a comparison based on e.g. the last fifty years would be better to compare differences between tracks.
Response:
We incorporated verbal descriptors of these terms in Figure 2 so as to not increase the length of the manuscript. Line 222.

Comment:
One of the principal difficulties is the comparison of statistics such as RI values between sites based on records of different length where the RI values are strongly related to survival of older individuals within the avalanche path. Perhaps a comparison based on e.g. the last fifty years would be better to compare differences between tracks.
Response:
We subset the period of record for each path from 1967-2017 and compared RI values. Nine paths exhibit no change in RI values when compared to the full record and one path RI values decreased by 4 years. We observed larger changes in the other two paths; JGO path where only one avalanche year was recorded (down from 5) and the median RI in LJC changed from 22.5 years to 35 years. We previously discussed JGO and LJC and the variable RIs of each of those paths in the Discussion. This exercise highlights that discussion emphasizing that these two paths were indeed slightly different than the others. We revised the text to illustrate that we examined the most recent 50 years to "scale" the return periods to account for loss of older trees. Methods (Lines 245-247), Results (Lines 352-356).

Comment:
No indication is given of the number of living vs dead trees sampled. If one discounts. the first 10 years of record over a third of the trees sampled have <35 years and half <60 years of record. How large/ tall are these trees on average at these ages and how might the nature of the tree-ring signal (i.e. the probability of recording a given event) vary with the age /height/ robustness of the tree. The avalanche chronologies are strongly biased towards the lifetime and response characteristics of the trees sampled. Although the number of GDs is cited in several places the breakdown of the individual types of GD e.g. scars, reaction wood series, TRD, tree mortality, etc. is never given.
Response:
We added # of living vs. dead trees sampled (line 292); 531 dead and 116 live sampled. Given the regulations of the protected areas in which we sampled, the majority of our cross sections were dead trees. The only exception is if the tree was growing a new leader and we sampled the old top that was previously destroyed in an avalanche. In addition, the dead trees spanned the same age class structure as the living trees from the surrounding forest and in the runout zone. Therefore, we did not bias the record by only working with dead trees. Rather, we simply improved the overall quality of the data by being able to work with cross sections. We would likely have obtained only lower quality responses by sampling more cores. Further, there were very few live trees/samples within the avalanche path itself and we sampled those that existed.

Comment:

In several cases the results are self evident- one gets better results from more sites, more trees, cross sections vs cores. The main strength is the regional and sampling approach. However, I have reservations about some of the derived statistics and the comparisons between individual records. There is little comment on the variability of the records within each of the sampling regions, or for example, the similarity between two adjacent paths. The main focus is the regional comparison. This regional approach tacitly assumes no significant differences in avalanche climate, or triggering factors across the region. There is no specific exploration of the relationship between avalanche activity and climatic factors.
Response:
In the discussion we provide interpretation on the variability between paths (e.g. JGO located east of the Continental Divide, LJC burned in the past, S10-7 sampled slightly differently than others b/c it was from another study). We also added text (lines 525-534) explaining inherent variability of RIs between individual paths for a variety of reasons. For example, avalanches are a function of weather and snowpack structure/variability. Climate drives weather but is not a first order effect on avalanche occurrence in any one given avalanche path. This is the motivation for this study. We derive a regional avalanche chronology to provide a spatial scale that aligns more with the spatial scale of climate drivers than any one individual path. On that note, an analysis of climate drivers of avalanche frequency is beyond the scope of this manuscript. Climate and regional avalanche relationships are the topic of a follow-on manuscript using this dataset that is currently undergoing peer-review.

Detailed and specific comments:
Comment:
52 delete semi-colon before bracket
Response:
Removed.

Comment:
66 Most of the data in table 2 is not greatly relevant to the paper. It is simply a compendium of earlier chronology studies. It is not used and could be in an appendix or supplementary material.
Response:
This table places our study in context to other studies re: spatial extent, sample size, # of GDs, etc. However, in an effort to decrease the length of our manuscript we moved it to Appendix A as Table A1.

Comment:
85-8 In this paper large magnitude avalanches are identified based on the cumulative evidence of disturbance by avalanches for an individual year in a given track given a minimum number of trees sampled. This identification is independent of the location of these disturbances within the individual avalanche track. The distribution of sampled trees within the avalanche track is therefore critical to the interpretation of this evidence with respect to avalanche hazard. Large magnitude in this scenario doesn't necessarily mean large or full length avalanches that would impact the runout/ danger zones. The authors need to emphasize more strongly that these avalanche chronologies are based on sampling in the terminal zone and down track margins and therefore the large magnitude events are inferred to be large full length avalanches that would represent hazard to these areas. In some cases there are a significant number of samples in the upper part of the track.
Response:
You are correct in that the definition of large magnitude avalanche in this study doesn't necessarily mean full length of avalanche path as we indeed sample at various locations in the runout zone and into the track in some instances. However, we sampled spatial extents within each avalanche path that represent large avalanches as defined in Greene et al. (2010). The areas sampled are representative of the runout extents of approximately ≥ size D3 avalanches. We also used recent (within previous 10 years) observed large magnitude avalanche activity in these paths to constrain the spatial extent of our sampling. We added this text (Lines 149-151).

Comment:
118 Figure 1 When enlarged Figure 1 clearly shows black dots which are assumed to be the sampling locations within the tracks. The figure caption should clearly point this out-it is not clear from the key and does not seem to be mentioned in the text or caption. As tree location is a critical factor in defining the size of avalanches their specific location is important. At several tracks the location of the sampled trees is some distance from the terminal zone of the avalanche track (there are two sampled areas on the northernmost GTSR site near Crystal Point?). Perhaps the track names should be identified on Figure 1.
Response:
We added more description in the figure caption in addition to the legend. As noted in the response above all sampling locations are within spatial extents representative of large magnitude avalanche extents. Line 111.

Comment:
Tables 2, 4 and 5. Is the colouring necessary?
Response:
We removed the color.

Comment:
110 These data do not appear to be used or referenced in the present study, even for comparative purposes. Did they identify similar major avalanche events?
Response:
These studies are referenced in the Intro. and Discussion (ca lines 137, 463, 487, 513, 571-572) and in current Table A1 for comparison of spatial extent, sample size, etc.

Comment:
160 the spatial footprint is 3000km2 in the abstract and 3500 km2 here.
Response:
Revised to read 3500 km^2 in the Introduction (ca. line 91).

Comment:
167 The text at this point suggests that all the cross sections were from dead trees and that the only living trees sampled were cored. Is this the case? Is the outer ring from these dead trees assumed to be from a "high magnitude" event i.e. the tree was killed/ sheared by an avalanche. These outer rings were presumably crossdated from adjacent living trees or chronologies. Were the core data actually used?
Response:
First, most cross sections were from dead trees. As previously mentioned, the only exception is if the tree was growing a new leader and we sampled the old top that was destroyed in an avalanche. The outer ring from these dead trees is not presumed to be from an avalanche as the tree may have died from some other cause and transported to the sampled location. We only dated the outer ring as an avalanche if historical records indicated a large magnitude avalanche in that path. The cross sections were indeed cross dated from living trees (i.e. cores) from either the adjacent gallery forest or nearby chronologies from the ITRDB (see Table A2). The core data were used for cross dating and for avalanche event dating if a signal was evident as some of these cores were sampled near the trim line where very large avalanches may have reached.

Comment:
200 + How does one also counter the censoring of the avalanche record due to continuing persistence of damage (e.g. reaction wood or TRD) in tree rings for several years following a major disturbance?

Response:
Cross sections provide us the ability to scrutinize reaction wood in any given location along the sample relative to other parts of the tree. Working with cross sections from all across the runout zone more or less ensures we don't miss avalanche events in years subsequent to a major slide event that damaged many trees. Subsequent slide events become obvious in trees that have recorded a major event already due to the generation of new scars and reaction wood growth that forms in different cardinal directions due to impacts from differing predominant flow directions. In addition, some proportion of trees in different parts of the runout zone that were not damaged in the prior slide event are likely to have captured the new event that occurred a year or two after the major event that was identified and classified. We see this throughout the record where individual avalanche events can and do classify as major slide event occurring in the same path but only a year or two after a different major event.
In addition to carefully classifying each signal (GD) in each sample using the classification scheme (see current Table 2), we also made the best attempt possible to filter out the the noise by using recent threshold methods devised by Corona et al. (2012) and Favillier et al. (2018, 2018)/Kogelnig Mayer (2011). The classification scheme clearly delineates that reaction wood or TRD alone receives a lower ranked classification. This then is taken into account in the W_{it} indexing process.

Comment:
212 responses within the tree or over the site?
Response:
The number of responses per year were calculated for each avalanche path. Descriptive statistics were computed for each path, sub-region, and region. We clarified the text to read: "We calculated the age of each tree sampled, the number of responses per year in each avalanche path, and computed descriptive statistics for the entire dataset." (lines 211-212)

Comment:
212-4 should the analyses and comparison of return intervals be limited to a common period when there is a reasonable sample of avalanche events (however defined) based on the age distribution of sampled trees within all tracks?
Response:
See response above to where we examined RIs from 1967-2017 as recommended with no major difference except in two paths. We previously discussed these paths in the Discussion.

Comment:
221 Figure 2 More information needs to be given in the caption identifying the symbols used N= sample trees available. GD= number of GDs identified. Perhaps include (N) after sample size in line 226. Is GD any GD or those above some minimal value? The context seems to indicate it is the number of GDs identified and not their magnitude.
Response:
We added text to the caption of Figure 2 (lines 222) and added "(N)" to line 228. GD is any growth disturbance identified and classified (as per Table 2) due to an avalanche.

Comment:
229 Is the statistic for avalanche years simply binary i.e. yes no?
Response:
Yes.

Commment:
239-40 therefore high magnitude years are all years where Wit is ≥3? Is the last term in Eqn 2 simply It? Essentially you derive a Wit value for each year for which there was avalanche data in each track and identify avalanche years as those with Wit ≥ 0.3.
Response:
We identify a large magnitude avalanche year as one where W_{it} is ≥2 (a measure of Medium and High confidence). The last term in Eq. 2 is indeed a typo. As we mentioned to Reviewer 1: We used the eqn. from Favillier et al. (2017, 2018) in the analysis, but accidentally inserted the R_t term from the Kogelnig-Mayer et al. (2011) eqn. in the manuscript. We revised the equation (line 235).

Comment:
Line 229 in the text indicates that RI calculations are based on the avalanche year examples (box 2 of fig 2) but lines 241 et seq. indicate that RI values are also calculated for high magnitude events (Wit ≥ 0.3) only. Therefore, are there two sets of RI data for (i) avalanche years and (ii) high magnitude (Wit) years? So which data are used in the subsequent analyses? Are these high magnitude years simply binary data (yes/no?)
Response:
The return intervals are simply calculated for large magnitude avalanches, the only type of avalanche investigated in this study. There is only one set of RI values for each path, sub-region, and region. The avalanche years are binary. We added text (lines 242-243) to clarify that the RIs used throughout the study are the ones calculated after all processing steps.

Comment:
253 RAAIt is based on the definition of avalanche years (It), not high magnitude Wit years. Therefore avalanche years are identified using the It statistic but high magnitude avalanches are identified using the Wit statistic. It appears that the RI data are calculated based on both the It and the Wit classification whereas the RAAIt statistics are based on the It definition of avalanche years. Is this correct?
Response:
The RAAI is based on the I_t index. The W_{it} is simply a threshold to identify confidence in the responses. Once again, this illustrates the benefit of using high quality cross sections where most of the avalanche years we identified for each path using the thresholds developed by Corona et al. (2012) fell above the W_{it} threshold.

Comment:
Line 324 seems to imply that the avalanche years identified in Figure 2 and the high magnitude events identified using Wit were identical so this difference does not matter? In any event only one set of calculations defining RI values should be specified. The term RI is used throughout the text but in places it is not clear whether it refers to the mean or median value.
Response:
We added text to clarify that we use median return interval throughout when referring to return interval (line 343).

Comment:
263 how does the probability of detection differ from the probability of avalanches?
Response:
The probability of detection (year) is a measure of the likelihood of detecting an avalanche year in the regional chronology by sampling any one given path and the probability of detection (path) is the probability of detecting the full chronology using any one given avalanche path. The probability of an avalanche would be the 1/RI (inverse of the return interval) for each individual path. These are both described in the revised Figure 2.

Comment:
284 are these comparisons included in this paper?
Response:
Yes. Line 350-351.

Comment:
291 ID by GD class but not type? So what was principal evidence used?
Response:
The GD class incorporates type in a systematic way for avalanche identification. Simply using type places imbalanced emphasis on certain types and not the cumulative signature of other types.

Comment:
298 this is predictable given the ages of trees sampled. Perhaps more interesting would be the years with the highest It values
Response:
The number of raw responses per year across all the paths is important as it provides a baseline to compare to avalanche years after applying signal:noise thresholds. The I_t values simply provide a % of responses based on the number of trees alive in each year per individual path. The I_t is simply used as a metric in the steps to identify avalanche years and doesn't serve to enhance the understanding of avalanche frequency when reported alone.

Comment:
299 Figures 3a and b appear identical and one is redundant. The scale on Fig 3b is incorrect (0.3 %?). The ages in Fig 3c indicate that many of these trees were quite small. What would the diameter of a 40-year old tree be? How does age influence the nature of the GD? In 3d were the larix and betula species identified?
Response:
We changed the figure (Figure 3) to have one panel with the proportions labeled on the bars instead of a second panel. We didn't measure the diameter of each tree/sample as it wasn't relevant to the study. The diameter of a 40-year old tree might vary from 20 cm to 60 cm, for example, depending on species, location, etc. Instead, we chose samples that would have the capability of recording an avalanche event. A smaller (perhaps younger if you equate age with size which isn't necessarily true in the northern Rockies) tree may be more pliable for a while so perhaps more resilient to impact pressure. Then as the tree grows (ages) it becomes more susceptible to uprooting by avalanches until it becomes larger (older). At that point the avalanche response on a larger tree is likely to be a scar or reaction wood. However, if the avalanche is sufficiently powerful, it will uproot the large tree. The Larix and Betula species were not identified given they were so few samples.

Comment:
308 missed 67 or 66?
Response:
Thanks for the catch. Changed to 67. Line 311.

Comment:
312 Figure 4 needs a scale. Some comparison of the derived GD data would be useful to make the point. To be effective this topic warrants a more extensive discussion and presentation of data than that presented here. This discussion and figure should probably be deleted.
Response:
We added a scale to Figure . The scale is also represented by the 5mm corer rectangles and mentioned in the caption. We believe that the results of this analysis in examining cores vs. cross-sections align with the objectives of the article. Determining the value of using cross-sections was central to the original

sampling design which distinguishes this study from previous dendro-avalanche research. The exercise must be mentioned in the Methods section because we present values on the comparisons in the Results and then the Discussion. Lastly, we provide this comparison to quantitatively illustrate the difference in using cross sections vs. cores and do not in any way discount any studies that use cores.

Comment:
312 More importantly were results from these cores actually used in the analysis.
Response:
These "cores" were simulated cores as if we indeed cored the sample as opposed to using the full cross section.

Comment:
324 Table 5 what does the standard deviation figure refer to (bottom line). Explain in caption?
Response:
It refers to the standard deviation of the return interval. We added text to the captions of Tables 3 and 4 to clarify this.

Comment:
332 Tables 4 and 5 What is the statistic 1/RI in these tables? Why is the median RI value used rather than the mean? Explain in the caption.
Response:
1/RI refers to the probability of an avalanche occurring in that avalanche path in any given year. We added text to the captions in Tables 3 and 4 to clarify this. We use the median as it is insensitive to outliers.

Comment:
334 Table 4 An additional line identifying the sub region should be added to the top of the table. The table should also give the period of record utilised to calculate RI for each track.
Response:
We added the line to current Table 3. We also added the period of record for each avalanche path. However, the POR for the return intervals was already listed and can be gleaned from avalanche years. The period of record (POR) for each path represents earliest inner year to the most recent outer year of all samples in the path. The RI was calculated on the return interval of avalanche years. This was added in the caption to current Table 3 (previous Table 4).

Comment:
337 JGO is a function of the early record but why LJB? LJB and LJC are 26, LGA is 25 and shed 7 is 28?
Response:
We don't really follow this comment. What are the values you reference for LJB, LJC, LGP (LGA [sic]) and S7? Those values aren't the RI for any of those paths.

Comment:
399 Table 7 explain MLC and HLC in the caption
Response:
Added text to updated Table 6. Line 415.

Comment:
346 Figure 6 what are the data plotted in this Figure? The median of GDO in Table 4 is ca 34 but in this figure it is ca 28. For LGP the median is ca 12.6 in Table 4 but ca 8 in figure 6
Response:

Figure 6 shows the return intervals for each path, sub-region, and overall region as stated in the caption. Good catch. There is one typo in Table 4 (new Table 3). The median for JGO (GDO [sic]) is 28.5. However, the median for LGP is listed as 8 in Table 4 and is also 8 in Figure 6.

Comment:
338-40 surely the similarities and differences between tracks reflect the length and nature of the avalanche record in each track? Differences/ similarity in return intervals are partially dependant on the length of record
Response:
As we demonstrated to your comment in the beginning of the review, "scaling" the period of record makes a difference in only the two paths that we already discuss as being different in terms of RI values. Here is the response to that original comment: We subset the period of record for each path from 1967-2017 and compared RI values. Nine paths exhibit no change in RI values when compared to the full record and one path RI values decreased by 4 years. We observed larger changes in the other two paths; JGO path where only one avalanche year was recorded (down from 5) and the median RI in LJC changed from 22.5 years to 35 years. We previously discussed JGO and LJC and the variable RIs of each of those paths in the Discussion. This exercise highlights that discussion that these two paths were indeed slightly different than the others. We added text to illustrate that we examined the most recent 50 years to "scale" the return periods to account for loss of older trees. Methods (Lines 245-247), Results (Lines 352-356).

Comment:
349-66 These differences in recurrence intervals are calculated for different periods of record. To be comparable do they need to be calculated over the same interval?
Response:
See response above and, yes, we compared a similar period of record.

Comment:
369 The avalanche records in these tracks start in 1933, 1936 and 1993so why compare them to a record starting in 1908 which presumably has avalanches predating those records. Surely comparisons need to be over the same intervals?
Response:
See response above.

Comment:
370 Figure 7 a nice (original?) way to show these data.
Response:
Thanks.

Comment:
380 Figure 8b the red line is not visible. Perhaps delete it and simply indicate this value in the caption
Response:
We kept the line and the value in the caption. It is a bit difficult to see (hopefully the indicated value in the caption helps), but readers are able to zoom in a bit when viewing on a monitor and it's clearly evident then and provides a graphical reference for readers.

Comment:
386 et seq. But the records being compared have quite different lengths and histories. How unique is the record of individual paths? If you compared the record of the tracks with similar length of record (say, ca 1950-2010, RMA-C, 54.3, LJA, 10.7 and S4.7) how similar are they?
Response:
See responses above re: comparison of similar lengths of record.

Comment:
405-6 These trends are mainly an effect of the increased sampling of avalanche years
Response:
Yes, these trends are likely a function of increasing samples through time which is why we mention them, but don't hang our hat on the trend results. The RAAI is simply another way to view a regional chronology using techniques from previous literature to allow for comparison.

Comment:
432-3 relevance of these comparisons?
Response:
As per Reviewer 1's comments we removed these lines as they aren't necessarily relevant.

Comment:
435 up into the bottom? English? Is the bottom the end or center of the track?
Response:
Revised sentence to read "However, at several sites we also collected samples into the bottom of the track (S10.7, Shed 7, and 1163) rather than just the runout zone." (lines 451-452). The bottom is the end of the track just above the runout zone.

Comment:
437-40 some specific dates needed here as this is the basis for the selection of records used. What specifically is the most recent time period for which you have adequate data across the network?
Response:
This sentence is a bit confusing so we revised to read: "Therefore, we chose to examine more recent time periods dictated by the avalanche years identified through the double threshold methods." (lines 457-458).

Comment:
451-2 how frequent is tree removal? What % of GDs are termination of growth vs other indicators of avalanche damage?
Response:
We don't really know the frequency of tree removal. It depends on the impact pressure of any given avalanche and this isn't something we can tease out from our data. It is not possible to determine the real % of GDs due to termination of growth because we can't assume the tree was killed by an avalanche for all of our dead and downed samples. Tree mortality could be caused by insects, storm damage, etc. and a subsequent avalanche could then transport the tree. However, if we assume that all sampled trees were removed by an avalanche (a rather large assumption), then we can take the number of cross sections (614) divided by the number of GD (2134). This provides a rough estimate under this assumption.
$\frac{614}{2134} \times 100 = 29\%$ of GDs are termination of growth.

Comment:
454 Although mentioned several times this incomplete historical record is never presented or directly compared to the equivalent tree-ring record for the comparable sites
Response:
We state in lines 141-143 that we compare the records for the 3 paths in JFS Canyon to this historical observational record but only for qualitative purposes. The record is simply used to provide some context for 3 avalanche paths. We reference Reardon et al. (2008) and that is where the observational record can be found. Text from Methods: "We compared the reconstructed avalanche chronology of the JFS sub-region to the historical record for qualitative purposes of large magnitude years. A quantitative comparison would not be reflective of the true reliability of tree-ring methods because of the incomplete historical record."

Comment:
475 the difference between Readon's earlier results or the other avalanche tracks? What are these differences?
Response:
We revised the sentence for clarity to "This is likely the root of the difference for S10.7 and the reason this path contains the largest numbers of avalanche years in this analysis." (lines 490-491).

Comment:
481 LJC has the greatest RI? It has the greatest median but not mean. The large median is a function of the small sample size in this track. The fire may have taken out evidence for most events between 1943 and 2017 and therefore this is not a valid comparison.
Response:
We revised the sentence to read "...were the greatest in this sub-region.." (line 506) as the RIs for JGO are the greatest. We agree that the fire played a major role in removing some evidence and now the slope is more exposed and susceptible to avalanching. We added text reflecting the fire's impact on data availability (lines 513-514).

Comment:
489 using which RI value, mean or median? What is the correlation statistic?
Response:
We compared both mean and median RI values. The results are for median. r=0.65, p=0.02, Figure A1. This was stated in the Results (line 350-351 previously lines 343-344).

Comment:
495 JGO is very unusual with only two avalanches between 1880 and 2017! The critical difference is the absence of documented events in the last 50 years. The only answer to these tentative explanations is more data from adjacent tracks. Perhaps the only comment necessary is that the reason for this is not known.
Response:
This path is unusual and we provide some explanation given its unique geographical location east of the Continental Divide within our dataset. We added text to reflect your very good points about this path (lines 498-499). "To understand if this value is accurate, we would have to sample adjacent tracks to determine if the return intervals are similar or not."

Comment:
507 but these differences are never explored
Response:
As previously mentioned, it is beyond the scope of this paper to explore the localized weather and climate drivers and the interaction with terrain. We explore such atmospheric and climate drivers in another manuscript.

Comment:
527 but these changes are also influenced by which avalanche track you remove.
Response:
The changes are only influenced by the removal (or addition) of the S10.7 path which we state and discuss in the next paragraph. We also reference recent literature that discusses the importance of selecting individual avalanche paths (line 553-554).

Comment:
532 But how typical is the record of s10-7 of other paths in the region see e.g. Table 4

Response:
We added text describing how S10.7 differs in line 554-556. “This is also illustrated by the large number of avalanche years detected in S10.7 due to increased sampling in the track.”

Comment:
533 s10.7 has the most avalanche activity but surprisingly is not compared with the available, if limited, observational record.
Response:
Reardon et al. (2008) provides a more detailed examination of the individual path S10.7 and by referencing their work we are able to focus on the effect to the overall regional chronology, the major objective of our study.

Comment:
538 What is an avalanche cycle chronology?
Response:
We changed text to be more clear. “...to reconstruct major widespread avalanche events.” (lines 560-562).

Comment:
547-9 these data would be useful here to validate some of these comments or are they solely based on the examples which follow.
Response:
They are based on the examples that follow.

Comment:
566 paths with one scar or one GD of class 3? Where are these scar data?
Response:
Good catch. We changed to “GD” (line 590). We referenced the data in Section 7 - Data Availability (line 657) (https://doi.org/10.5066/P9TLHZAI, 2019)

Comment:
570 is the sample design or the number of paths the critical factor here? The sample design clearly increases the area covered.
Response:
We discuss that sampling more paths certainly increases the POD of avalanche years. However, the sampling design using scale triplet allows one to scale the process of avalanching from small path scale to the larger regional scale.

Comment:
582-5 Basic point is that if you sample more avalanche tracks you get more avalanche years and a more consistent pattern may emerge. However, the pattern of avalanche activity varies from track to track and from year to year.
Response:
Correct. This illustrates the benefit of such a sampling design where one can scale the process across spatial extents.

Comment:
587 Is this a function of sample size or other characteristics such as the time period covered by those samples and the sampling network?
Response:
A function of sample size. We collected a large number of samples across the region, but at the individual path scale, more would have been better in two of the paths.

Comment:
603 this median value probably should be linked to a time frame to which it applies
Response:
We added the full regional chronology period of record (1866-2017) (line 626).

Comment:
Figure A1 What are the data used here (reference to Table 2)? Some numbers are barely visible. Perhaps use bolder (larger) numbers and colour as a background to individual cells?
Response:
Yes, the data refer to Table 2 (new Table 1). We revised Figure A1 with larger numbers and a different background for easier readability.

A regional spatio-temporal analysis of large magnitude snow avalanches using tree rings

Erich Peitzsch[1,2*], Jordy Hendrikx[2], Daniel Stahle[1], Gregory Pederson[1], Karl Birkeland[3,2], and Daniel Fagre[1]

[1] U.S. Geological Survey Northern Rocky Mountain Science Center, West Glacier, Montana, USA
[2] Snow and Avalanche Lab, Department of Earth Sciences, Montana State University, Bozeman, Montana, USA
[3] U.S.D.A. Forest Service National Avalanche Center, Bozeman, Montana, USA

*epeitzsch@usgs.gov, 215 Mather Dr., West Glacier, MT, USA, 59936

Abstract. Snow avalanches affect transportation corridors and settlements worldwide. In many mountainous regions, robust records of avalanche frequency and magnitude are sparse or non-existent. However, dendrochronological methods can be used to fill this gap and infer historic avalanche patterns. In this study, we developed a tree-ring based avalanche chronology for large magnitude avalanche events ($\geq$ *~size D3*) using dendrochronological techniques for a portion of the northern United States Rocky Mountains. We used a strategic sampling design to examine avalanche activity through time and across nested spatial scales (i.e. from individual paths, four distinct sub-regions, and the region). We analysed 673 total samples from 647 suitable trees collected from 12 avalanche paths, from which 2,134 growth disturbances were identified over years 1636 to 2017 Common Era (C.E.). Using existing indexing approaches, we developed a regional avalanche activity index to discriminate avalanche events from noise in the tree-ring record. Large magnitude avalanches common across the region occurred in 30 individual years and exhibited a median return interval of approximately three years (mean = 5.21 years). The median large magnitude avalanche return interval (3-8 years) and the total number of avalanche years (12-18) vary throughout the four sub-regions, suggesting the important influence of local terrain and weather factors. We tested subsampling routines for regional representation, finding that sampling eight random paths out of a total of 12 avalanche paths in the region captures up to 83% of the regional chronology, whereas four paths capture only 43% to 73%. The greatest value probability of detection for any given path in our dataset is 40% suggesting that sampling a single path would capture no more than 40% of the regional avalanche activity. Results emphasize the importance of sample size, scale, and spatial extent when attempting to derive a regional large magnitude avalanche event chronology from tree-ring records.

Commented [EP1]: As per Reviewer 1 (Favillier) we made numerous changes to simplify and clarify the writing for better readability throughout the manuscript but especially in the Results and Discussion. Some of those changes aren't reflected in the markup version so as to avoid clutter.

1 Introduction

1.1 Background

Snow avalanches are hazardous to human safety and infrastructure (Mock et al., 2016; Schweizer, 2003) as well as an important landscape disturbance affecting mountain ecosystems (Bebi et al., 2009). In the United States an average of 27 people die in avalanche accidents each winter (CAIC, 2020). Avalanches, especially large magnitude events, also affect transportation corridors and settlements throughout the world. For example, avalanches impact numerous roadways and railroad corridors in the western United States (Armstrong, 1981; Hendrikx et al., 2014; Reardon et al., 2008). Consequently, understanding general avalanche processes and associated large magnitude avalanche return intervals is critical for local and regional avalanche forecasters, transportation agencies, and land use planners.

Long-term, reliable, and consistent avalanche observation records are necessary for calculating avalanche return intervals which can be used in infrastructure planning and avalanche forecasting operations. However, such records are often sparse or non-existent in many mountainous regions, including areas with existing transportation corridors. Thus, inferring avalanche frequency requires the use of dendrochronological methods to document damaging events or geomorphic response within individual trees at individual path to regional scales. Even in regions with historical records, tree-ring dating methods can be used to extend or validate uncertain historical avalanche records, which has led to the broad implementation of these methods in mountainous regions throughout the world (e.g. Corona et al., 2012; Favillier et al., 2018; Schläppy et al., 2014) .

Numerous studies reconstructed avalanche chronologies in the United States using tree-ring methods (Burrows and Burrows, 1976; Butler et al., 1987; Carrara, 1979; Hebertson and Jenkins, 2003; Potter, 1969; Rayback, 1998). Butler and Sawyer (2008) provided a review of current methodologies and types of tree-ring responses used in avalanche dendrochronological studies. Favillier et al. (2018) provided a more recent comprehensive graphical summary of dendrochronological avalanche studies throughout the world. Numerous studies used dendrochronological techniques to develop avalanche chronologies for remote regions without historical avalanche records or areas with inconsistent avalanche observations (Butler and Malanson, 1985a; Germain et al., 2009; Reardon et al., 2008; Šilhán and Tichavský, 2017; Voiculescu et al., 2016), and many studies used these techniques to examine avalanches across space and time (Table A1).

1.2 Framework and objectives

Tree-ring avalanche research is resource and time intensive. Like other scientific fields, it is not feasible to completely sample the variable of interest with infinite detail due to logistical and financial constraints (Skøien and Blöschl, 2006). Thus, a strategic spatial sampling method is necessary. Here, we strategically sampled 12 avalanche paths in four distinct sub-regions of the U.S. northern Rocky Mountains of northwest Montana to examine spatial differences at a regional scale. The sampling strategy is based on the concept of

Deleted: ;)

Deleted: 1

Moved down [1]: : List of previous avalanche-dendrochronological work *with more than one avalanche path* in study – to place our regional work in context with other regional/multiple path studies. Number of samples, paths, growth disturbances (GD), and spatial extent (linear distance between most distant avalanche paths in study area) are included. For spatial extent, *NA* is reported in studies where spatial extent is not reported or could not be inferred from maps in the published work. Where spatial extent is not reported directly in previous work, it is estimated by using maps from the published work and satellite imagery.¶

Deleted: ¶
Authors ... [1]

Moved down [2]: Authors

scale triplet, which defines the spacing, extent, and support of our sampling scheme (Blöschl and Sivapalan, 1995). Incorporating the scale triplet concept helps us understand the nature of the problem, the scale at which measurements should be made, and how we can estimate the measurements across space. Often, the scale at which samples are collected differs from the scale necessary for predictive purposes (Blöschl, 1999). For example, if we are interested in avalanche frequency relationships with regional climate patterns but tree-ring samples are collected at an avalanche path scale, then a network of sampled paths need to be spaced and aggregated across the core of the climatically similar region. In our study, the extent is the entire region and sub-regions, the spacing is the distance between avalanche paths and sub-regions, and the support is the size of the area being sampled. In addition, the process scale is the natural variability of avalanche frequency, the measurement scale is the tree-ring proxies used to represent avalanche occurrence on an annual temporal scale, and the model scale relates to aggregating all of the sample areas to derive a regional avalanche chronology.

We adopt Germain's (2016) definition that large magnitude avalanches are events characterized by low and variable frequency with a high capacity for destruction. This generally translates to a size 3 or greater on the destructive classification scale - i.e. ability to bury or destroy a car, damage a truck, destroy a wood frame house, or break a few trees (Greene et al., 2016).

Understanding the spatiotemporal behavior of large magnitude avalanches on the regional scale will improve avalanche forecasting efforts, especially for operations involving avalanche terrain that impacts transportation corridors. Here, we aim to answer three specific questions:

1) What is the regional, sub-regional, and path specific frequency of large magnitude avalanches in the U.S. northern Rocky Mountains of northwest Montana?

2) How does the spatial extent of the study region affect the resultant avalanche chronology?

3) What is the probability of detecting regional avalanche activity by sampling different avalanche paths?

To our knowledge, this is the first study to look at how various spatial scales compare when reconstructing a regional avalanche chronology from dendrochronological data on a large dataset (N > 600 samples). Further, we believe this is the first study that utilizes a regional dendrochronological record to derive return periods over a large (> 3500 km^2) spatial extent. Our hypothesis is that aggregating the paths into sub-region and then again into a full region allows us to minimize the limitation of tree-ring avalanche chronologies underestimating avalanche years at these scales.

Deleted: 3000

2. Methodology

2.1 Study Site

Our study site consists of 12 avalanche paths in the Rocky Mountains of northwest Montana, USA (Figure 1 and Table 1). We sampled sets of three avalanche paths in four distinct sub-regions within three mountain ranges: the Whitefish Range (WF, Red Meadow Creek) and Swan Range (Swan, Lost Johnny Creek) on the

Deleted: 2

Flathead National Forest, and two sub-regions within the Lewis Range in Glacier National Park (GNP), Montana. The sites in GNP are along two major transportation corridors through the park: the Going-to-the-Sun Road (GTSR) and U.S. Highway 2 in John F. Stevens (JFS) Canyon. These two areas were utilized for previous dendrochronological avalanche research (Butler and Malanson, 1985a; Butler and Malanson, 1985b; Butler and Sawyer, 2008; Reardon et al., 2008). A robust regional avalanche chronology reconstruction will help place the previous work in context of the wider region. The other two sites, WF and Swan, are popular backcountry recreation areas with access via snowmachine in the winter along a U.S. Forest Service road. The avalanche paths in each sub-region encompass a range of spatial extents from adjacent (i.e. < 30 m apart) to ~10 km apart. Overall, this study region provides an ideal natural setting for studying avalanches due to its geography, inclusion of transportation and recreation corridors potentially impacted by avalanches, relative accessibility, and no artificial avalanche hazard mitigation.

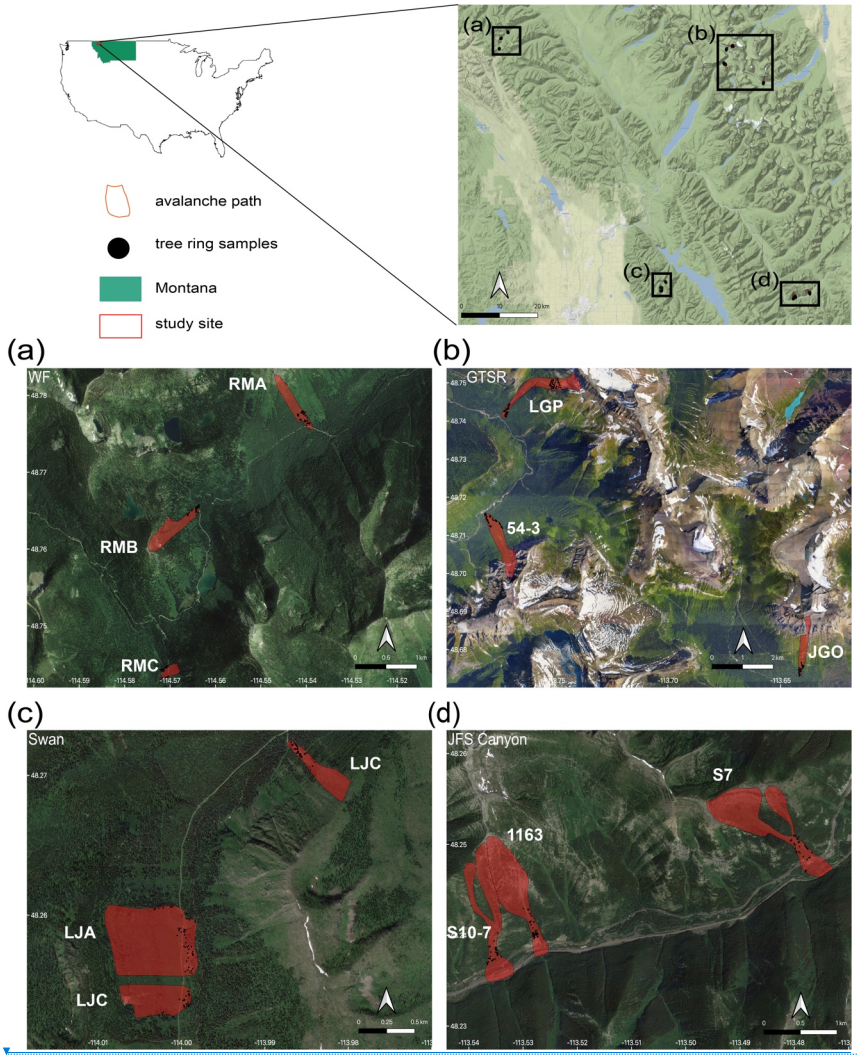

Deleted:

avalanche path
tree ring samples
Montana
study site
(a)
WF
(c)
Swan

Figure 1: Study site. The red rectangle in the state of Montana designates the general area of the four sampling sites. The sites are (A) Red Meadow, Whitefish Range (WF), (B) Going-to-the-Sun Road (GTSR), central GNP, (C) Lost Johnny Creek, northern Swan Range (Swan), and (D) John F. Stevens Canyon (JFS), southern GNP. Black dots represent sample locations. Abbreviated names of each path are in white text adjacent to red polygons. Satellite and map imagery: © Google (n.d.). Maps produced using ggmap in R (Korpela et al. 2019).

Table 1: Topographic characteristics of all avalanche paths. * denotes two major starting zones for one runout in Shed 10-7 and Shed 7 paths.

Path	Trees (n)	Full Path Elev. (mean) (m)	Full Path Elev. (range) (m)	Starting Zone Elev. (mean) (m)	Full Path Slope (mean) (°)	Starting Zone Slope (mean) (°)	Median Aspect (°)	Area (km^2)	Length (m)	Vertical (m)	Years of previous fire or logging
WF-Red Meadow A (RMA)	41	1651	1462 - 1957	1774	26	32	155	0.32	1004.97	495.20	1952
WF-Red Meadow B (RMB)	40	1870	1643 - 2164	1965	31	37	53	0.13	1041.98	521.27	1967
WF-Red Meadow C (RMC)	42	1650	1582 - 1742	1692	28	33	257	0.08	326.14	160.46	1962
GTSR - 54-3	56	1501	1080 - 2149	1708	31	40	327	0.44	2063.61	1068.49	NA
GTSR-Little Granite (LGP)	109	1770	1109 - 2314	2170	24	34	250	0.78	2940.29	1205.07	NA
GTSR-Jackson Glacier Overlook (JGO)	41	1863	1500 - 2660	2090	32	42	180	0.70	1793.13	1159.84	NA
Swan-Lost Johnny A (LJA)	53	1619	1441 - 1896	1731	29	38	77	0.41	811.50	455.27	1971-72
Swan-Lost Johnny B (LJB)	26	1633	1478 - 1879	1721	32	39	76	0.57	617.52	401.80	1971-72
Swan-Lost Johnny C (LJC)	42	1550	1344 - 1750	1670	34	36	326	0.39	667.88	405.66	1957, 2003
JFS-Shed 10-7 (S10.7)*	109	1644	1233 - 2193	1910 1964	31	35 39	176	0.13	1745.66	959.74	1910
JFS-Shed 7 (S7)*	46	1712	1310 - 2078	1935 1837	29	34 36	152	0.57	1686.96	768.01	1910
JFS-1163	50	1718	1250 - 2217	1861	38	42	158	0.17	1636.52	966.82	1910
All Paths	655	1690	1080 - 2660	1869	-0.17	0.14	31	37	Spatial footprint = 3500 km^2		

Deleted: 2

Deleted: Different colors indicate sub-regions as shown in Figure 1. …

Northwest Montana's avalanche climate is classified as both a coastal transition and intermountain avalanche climate (Mock and Birkeland, 2000), but it can exhibit characteristics of both continental or coastal climates. The elevation of avalanche paths within the study sites range from approximately 1100 m to 2700 m and the starting zones of these paths are distributed among all aspects (Table 1).

Deleted: 2

We eliminated or minimized influence from exogenous disturbance factors such as logging and wildfire by referencing wildfire maps extending back to the mid-20th century. We selected sites undisturbed by wildfire since this time except for Lost Johnny Creek, which was purposeful as this area burned most recently in 2003. We also minimized the influence of logging by selecting sites not previously logged. Using historical logging parcel spatial data, we determined logging in some sites was limited to very small parcels adjacent to the farthest extent of the runout zones.

The historical observational record in this area is limited. In this study region, the Flathead Avalanche Center (FAC), a regional U.S. Forest Service backcountry avalanche center, records all avalanches observed and reported to the center. However, not all avalanches are observed or reported given the approximately 3500 km^2 advisory area. The Burlington-Northern Santa Fe Railway (BNSF) Avalanche Safety Program records most avalanches observed in John F. Stevens Canyon in southern Glacier National Park, where there is 16 km of rail line with over 40 avalanche paths. However, systematic operational observations only began in 2005. Observations prior to this time are inconsistent, though large magnitude avalanches were mostly recorded. Reardon et al. (2008) developed as complete a record as possible from the Department of Transportation and railroad company records, National Park Service ranger logs, and popular media archives. In this sub-region, avalanche mitigation is conducted on an infrequent and inconsistent basis in emergency situations, which is typically only once a year, if at all. Thus, the record approximates a natural avalanche record. We compared the reconstructed avalanche chronology of the JFS sub-region to the historical record for qualitative purposes of large magnitude years. A quantitative comparison would not be reflective of the true reliability of tree-ring methods because of the incomplete historical record.

2.2 Sample Collection and Processing

Our sampling strategy targeted an even number of samples collected from both lateral trimlines at varying elevations and trees located in the main lower track and runout zone of the selected avalanche paths. This adequately captured trees that were destroyed and transported, as well as those that remained in place. The definition of large magnitude avalanche in this study refers to avalanches of approximately size D3 or greater (Greene et al. 2010) and may not run the full length of the avalanche path. We sampled spatial extents within each avalanche path representative of runout extents ≥ size D3 avalanches. We also used recent (within previous 10 years) observed large magnitude avalanche activity in these paths to constrain our sampling.

Sample size for avalanche reconstruction using tree-ring data requires careful consideration. Butler and Sawyer (2008) suggest that a few damaged trees may be sufficient for avalanche chronologies, but larger target sample sizes increase the probability of detecting avalanche events (Corona et al., 2012). Germain et

al. (2010) examined cumulative distribution functions of avalanche chronologies and reported only slight increases in the probability of extending chronologies with sample size greater than 40. Thus, given the large spatial footprint (~3500 km^2) of this study and feasibility of such a large sample size, we sampled between 26-109 samples per avalanche path resulting in 655 trees (Table 2). Eight trees were unsuitable for analysis leaving us with 673 total samples from 647 trees. Of the 673 total samples, we collected 614 cross sections and 59 cores. Shed 10.7 (S10.7) path was the focus of previous work (Reardon et al., 2008), and the dendrochronological record extends up to 2005 (n=109 trees). Little Granite Path (LGP) was collected in the summer of 2009 (n=109 trees). We sampled the remaining 10 paths (437 of the 655 total trees) in the summer of 2017.

We collected three types of samples: (1) cross sections from dead trees, (2) cross sections from the dead leaders of avalanche-damaged but still living trees, and (3) cores from living trees. We used predominantly cross-sections in this study for a more robust analysis as events can potentially be missed or incorrectly identified in cores. We emphasized the selection of trees with obvious external scars and considered location, size, and potential age of tree samples. A limitation of all avalanche dendrochronology studies is that large magnitude events cause extensive damage and high tree mortality, thereby reducing subsequent potential tree-ring records.

We sampled stem cross-sections at the location of an external scar or just above the root buttress from downed or standing and dead trees, and from stems of trees topped by avalanche damage. We extracted tree-ring core samples from live trees with obvious scarring or flagging along the avalanche path margins and runout zone using a 5 mm diameter increment borer. We collected a minimum of two and up to four core samples per tree (two in the uphill-downhill direction and two perpendicular to the slope). We photographed each sample at each location and recorded species, GPS coordinates (accuracy 1-3 m), amount of scarring on the cambium of the tree, relative location of the tree in the path, and upslope direction (Peitzsch et al., 2019). We also recorded location characteristics that identified the tree to be in-place vs. transported from its original growth position (i.e. presence or absence of roots attached to the ground or the distance from an obvious excavated area where the tree was uprooted).

To prevent radial cracking and further rot, we dried and stabilized the cross sections with a canvas backing. We sanded samples using a progressively finer grit of sandpaper to expose the anatomy of each growth ring, and used the visual skeleton plot method to account for missing and false-rings and for accurate calendar year dating (Stokes and Smiley, 1996). We assessed cross-dating calendar-year accuracy of each sample and statistically verified against measured samples taken from trees within the gallery forest outside the avalanche path, and from preexisting regional chronologies (Table A2) (ITRDB, 2018) using the dating quality control software COFECHA (Grissino-Mayer, 2001; Holmes, 1983). For further details on cross-dating methods and accuracy calculation for this dataset see Peitzsch et al. (2019).

Deleted: full stem

Deleted: -

Deleted: (both downed and standing dead)

Deleted: and

Deleted: live

Deleted:

Deleted: stumps

Deleted: 1

2.3 Avalanche Event Identification

We analyzed samples for signs of traumatic impact events (hereafter "responses") likely caused by snow avalanches. We adapted a classification system from previous dendrogeomorphological studies to qualitatively rank the trauma severity and tree growth response from avalanche impacts using numerical scores ranked 1 through 5 (Reardon et al., 2008). This classification scheme identified more prominent avalanche damage responses with higher quality scores, and allowed us to remain consistent with previous work (Corona et al., 2012; Favillier et al., 2018) (Table 2). To compare our ability to capture avalanche trauma events using cores versus those captured using cross-sections, we sampled a subset (n=40) of the cross-sections by analyzing four 5 mm wide rectangles to mimic a core sample from an increment borer. The four subsamples on each cross section were made perpendicular to one another (i.e. 90 degrees) based on the first sample taken from the uphill direction of each stem to replicate common field sampling methods. We then summarized results from the four subsamples for each tree by taking the highest response score for each growth year. Finally, we compared the number, quality response category, and calendar year of the avalanche trauma events derived from the core subsamples to those identified from the full cross sections.

Deleted: 3

Deleted: /

Deleted: /

Table 2: Avalanche impact trauma classification ratings.

Deleted: 3

Classification	Description
C_1	• Clear impact scar associated with well-defined reaction wood, growth suppression or major traumatic resin duct development. • Or, the strong presence of some combination of these major anatomical markers of trauma and growth response recorded in multiple years of growth and occurring at a year that multiple samples from other trees at the site record similar trauma and scaring. • C_1 events are also assigned to the death date of trees killed by observed avalanche mortality at the collection site; the presence of earlywood indicates an early spring, or late avalanche season, event killed the tree.
C_2	• Scar or small scar recorded in the first ten years of tree growth without associated reaction wood, growth suppression or traumatic resin ducts. • Or, obvious reaction wood, growth suppression or significant presence of traumatic resin ducts that occur abruptly after normal growth that lasts for 3 or more years.
C_3	• The presence of reaction wood, growth suppression, or traumatic resin ducts recorded in less than 3 successive growth years.
C_4	• Poorly defined reaction wood, growth suppression or minimal presence of traumatic resin ducts lasting 1-2 years. • Or, a C_3 class event occurring in the first 10 years of tree growth where the cause of damage could result from various biological and environmental conditions.
C_5	• Very poorly defined reaction wood, growth suppression, or minimal presence of traumatic resin ducts isolated in one growth year. • Or, a C_4 class event occurring in the first 10 years of tree growth where the cause of damage could result from various biological and environmental conditions.

2.4 Chronology and Return Period Calculation

To generate avalanche event chronologies and estimate return periods for each path and for the entire study site, we utilized *R* statistical software and the package *slideRun*, an extension of the *burnR* library for forest fire history data (Malevich et al., 2018). We calculated the age of each tree sampled and the number of responses per year in each avalanche path, and computed descriptive statistics for the entire dataset. Estimates of avalanche path return intervals should be viewed as maximum return interval values due to the successive loss of samples and decreasing sample number back through time.

We used a multi-step process to reconstruct avalanche chronologies on three different spatial scales: individual paths, four sub-regions, and the entire region. We also calculated a regional avalanche activity index (RAAI) (Figure 2). The process involved first calculating the ratio of trees exhibiting GD over the number of samples alive at year *t* to provide the index I_t (Shroder, 1978):

$$I_t = \left(\frac{\sum_{i=1}^{n}(R_t)}{\sum_{i=1}^{n}(A_t)}\right) \times 100 \quad (1)$$

where *R* is the number of trees recording a GD at year *t* with A_t representing the number of trees alive in our samples at year *t*.

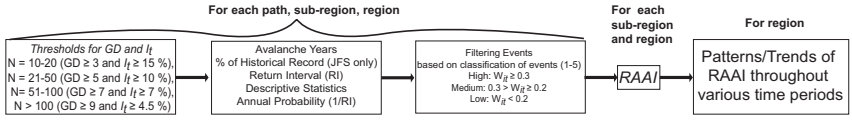

I_t (Eq. 1)	This index provides an indication of the number of GD per samples alive in any given year (Schroder, 1978).
W_{it} (Eq. 2)	A weighted index factor that accounts for the class of each GD (Favillier et al., 2017, 2018).
$RAAI_t$ (Eq. 3)	A regional avalanche activity index per year (Germain et al. 2009).
POD_{year} (Eq. 4)	The probability of detecting an avalanche year in the regional chronology by sampling any given individual path.
POD_{path} (Eq. 5)	The probability of detecting the full regional chronology using any one given path's chronology.

Figure 2: General workflow of analytical methods to reconstruct regional avalanche chronology and regional avalanche activity index. N=sample size. GD=growth disturbances. I_t= Index of ratio of responses to tree alive. RI=return interval. W_{it}=weighted index as per Favillier (2017,2018). RAAI=regional avalanche activity index as per (Germain et al. 2009). See Eqs. 1-5 for details.

We then used double thresholds to estimate the minimum absolute number of GD and a minimum percentage of samples exhibiting GD per year (I_t) based on sample size (N) following thresholds established by Corona et al. (2012) and Favillier et al. (2018): N = 10-20 (GD ≥ 3 and I_t ≥ 15 %), N = 21-50 (GD ≥ 5 and I_t ≥ 10 %), N= 51-100 (GD ≥ 7 and I_t ≥ 7 %), and N > 100 (GD ≥ 9 and I_t ≥ 4.5 %).

We then used the chronologies derived from this process to calculate a weighted index factor (W_{it}). We used this established threshold approach since it has been broadly employed in the literature and allows comparability of our avalanche chronology to results reported in other studies. We adapted previous equations of a weighted response index (Kogelnig-Mayer et al., 2011) to our 5-scale ranking quality classification to derive the W_{it}:

Deleted: and

Deleted: and

Deleted:

Deleted: We then estimated the number of avalanche years, descriptive statistics for return intervals (RI), and the annual probability (1/RI) for each path, sub-region, and region.

Deleted:

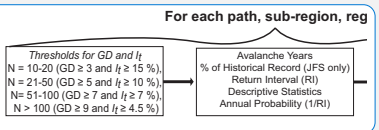

$$W_{it} = \frac{\left(\left(\sum_{i=1}^{n} T_{C_1} * 7\right) + \left(\sum_{i=1}^{n} T_{C_2} * 5\right) + \left(\sum_{i=1}^{n} T_{C_3} * 3\right) + \left(\sum_{i=1}^{n} T_{C_4,C_5}\right)\right)}{\sum_{i=1}^{n} A_t} \quad (2)$$

where the sum of trees with scars or injuries (C_1 - C_5) were multiplied by a factor of 7, 5, 3, 1 and 1 respectively (Kogelnig-Mayer et al., 2011).

Next, we classified W_{it} into high, medium, and low confidence events using the thresholds detailed in Favillier et al. (2018), where High: $W_{it} \geq 0.3$, Medium: $0.3 > W_{it} \geq 0.2$, Low: $W_{it} < 0.2$. This provided another step discriminating the avalanche events/years signal from noise. We included all events with medium to high confidence in the next analysis. We then estimated the number of avalanche years, descriptive statistics for return intervals (RI), and the annual probability (1/RI) for each path, sub-region, and region. We use the RI derived after filtering events for confidence as the intervals throughout the study. We then compared return intervals for all individual paths and sub-regions using analysis of variance (ANOVA) and Tukey's Honest Significant Difference (HSD) (Ott and Longnecker, 2016). In the final step of analysis of RI we subset the period of record for each path from 1967-2017 to compare RI from this shortened time series to the full period of record for each path.

Next, we compared the number of avalanche years and return periods identified in the full regional chronology to subsets of the region to determine the number of paths required to replicate a full 12-path regional chronology. We assessed the full chronology against a subsampling of 11 total paths by sequentially removing the three paths with the greatest sample size. We then randomly sampled two paths from each sub-region for a total subsample of eight paths, followed by generating a subsample of four paths by choosing the path in each sub-region with the greatest sample size. Finally, we selected a random sample of one path from each sub-region to compare against a total of four single path subsamples.

2.5 Regional Avalanche Activity Index and Probability of Detection

Next, we used the I_t statistic from each path to calculate a regional avalanche activity index (RAAI) for the sub-regions and overall region (Germain et al., 2009). The RAAI for each year across the sub-regions and region provides a more comprehensive assessment of avalanche activity within the spatial extent. For each year t, we calculated RAAI:

$$RAAI_t = \left(\sum_{i=1}^{n} I_t\right) \Big/ \left(\sum_{i=1}^{n} P_t\right) \quad (3)$$

where I is the index factor as per Eq. (1) for a given avalanche path for year t and P is the number of paths that could potentially record an avalanche for year t. For the calculation of the overall RAAI, we required each path to retain a minimum sample size of ≥ 10 trees with a minimum number of three paths for year t, and a minimum of one path from each sub-region. We performed a sensitivity test to establish the minimum number of paths necessary to calculate an RAAI value for any given year.

Deleted: $W_{it} = \left(\left(\sum_{i=1}^{n} T_{C_1} * 7\right) + \left(\sum_{i=1}^{n} T_{C_2} * 5\right) + \left(\sum_{i=1}^{n} T_{C_3} * 3\right) + \left(\sum_{i=1}^{n} T_{C_4,C_5}\right)\right) * \frac{\sum_{i=1}^{n} R_t}{\sum_{i=1}^{n} A_t}$

Formatted Table

Deleted: For this subset of higher-quality events, we calculated

Deleted: ,

Deleted: avalanche

Deleted: overall

We also calculated the probability of detecting an avalanche year identified in the regional chronology as if any given individual path was sampled. The probability of detection for a given year (POD_{year}) is defined as:

$$POD_{year} = \frac{a}{a+b} \quad (4)$$

where a is the number of individual avalanche paths that identify any given avalanche year in the regional chronology and b is the total number of avalanche paths (n=12). We calculated POD_{year} for every year in the regional avalanche chronology. We then compared the POD_{year} of individual paths to the number of active avalanche paths as defined in Eq. (3).

We also calculated the probability of detection for each path for the period of record (POD_{path}):

$$POD_{path} = \frac{c}{c+d} \quad (5)$$

Deleted: 4

where c is the number of years identified in any given path that is included in the regional chronology and d is the number of years in the regional chronology that are not identified in the chronology for the given path. Finally, we examined trends in the RAAI through time using the non-parametric modified Mann-Kendall test for trend (Mann, 1945;Hamed and Rao, 1998). We parsed the dataset into four periods to allow comparability due to the loss of evidence and a decreasing sample size going back in time: the entire period of record, 1933 to 2017, 1950 to 2017, and 1990 to 2017. We selected these time periods based on the years with greatest responses and peak RAAI values (1933, 1950, and 1990). We excluded intervals after 1990 to retain a minimum of ~30-year record.

2.6 Geomorphological characteristics

Using a 10 m digital elevation model (DEM), we calculated a number of geomorphological characteristics for each path, including mean elevation (m, full path and starting zone), elevation range (m), eastness ($\sin(aspect)$) and northness ($\cos_{(aspect)}$) (radians), slope (degrees, full path and starting zone), curvature (index (0-1), profile and planform), roughness (index, full path and starting zone), perimeter (km^2), area (km^2), length (m), and vertical distance from starting zone to runout zone (m). We also calculated the mean of these characteristics for all paths in the region. The geomorphological characteristics allowed for a determination of the representativeness of the region as a whole (i.e. are the paths similar across the region?) as well as a comparison of the return interval for each path relative to these characteristics. Finally, we estimated the potential relationship between path length, starting zone slope angle, the number of avalanche years, and median return interval for each individual path using the Pearson correlation coefficient.

3. Results

We collected a total of 673 samples from 647 suitable avalanche impacted or killed trees (trees: n = 531 dead; n = 116 living) in the full 12-path regional avalanche collection. Of those 673 samples, 614 were cross sections (91%) and 59 were cores (9%). Within these samples we identified 2134 GD, of which 1279 were

classified as C_1 and C_2 (60%) (Figure 3(a and b)). The oldest individual tree sampled was 367 years, and the mean age of all samples was 73 years (Figure 3(c)). The period of record of sampled trees extended from 1636 to 2017 C.E. The most common species in our dataset was *Abies lasciocarpa* (*ABLA*, sub-alpine fir) (46%) followed by *Pseudotsuga menziesii* (*PSME*, Douglas-fir) (37%) and *Picea engelmannii* (*PIEN*, Engelmann spruce) (14%) (Figure 3(d)). The oldest GD response dates to year 1655. In the entire dataset, the five years with the greatest number of raw GD responses were 2002 (165 responses), 2014 (151 responses), 1990 (93 responses), 1993 (90 responses), and 1982 (75 responses).

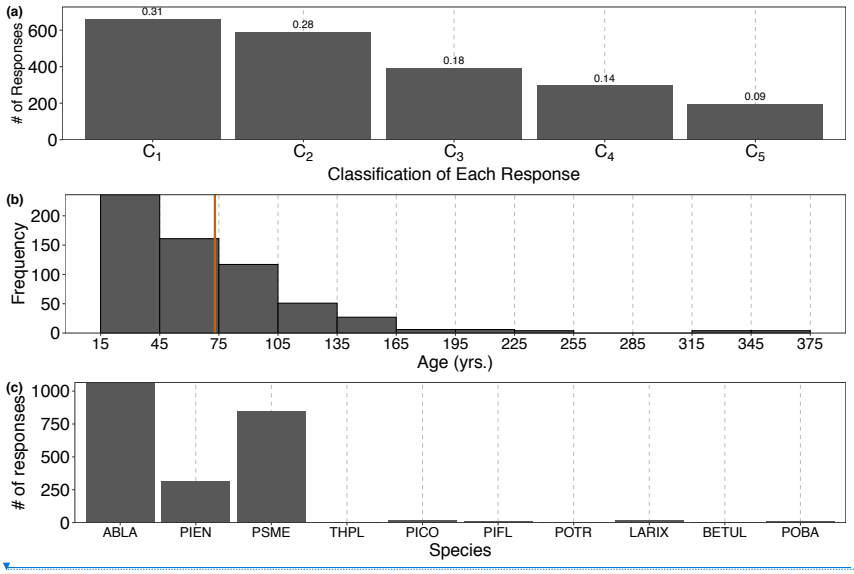

Figure 3: Histograms of (a) number of classification of responses (number above bar represents proportion), (b) sample age (red line represents mean age), and (c) species. For species: ABLA=*Abies Lasciocarpa*, PIEN = *Picea engelmannii*, PSME = *Pseudotsuga menziesii*, THPL = *Thuja plicata*, PICO = *Pinus contorta*, POTR = *Populus tremuloides*, LARIX = *Larix* Mill., BETUL = *Betul* L., POBA = *Populus balsamifera*.

3.1 Avalanche Event Detection: Cores versus Cross-Sections

The avalanche event subset analysis that compared results as if samples were from cores versus full cross sections showed that core samples alone would have missed numerous avalanche events and generated a greater proportion of low-quality growth disturbance classifications (Figure 4). For the subset of 40 samples analyzed as cores we identified only 124 of 191 (65%) total GD. Of the 67 GDs that we would have missed just by using cores, 24 were classified as C_1 quality events, 24 were C_2, 14 were C_3, 3 were C_4, and 2 were C_5.

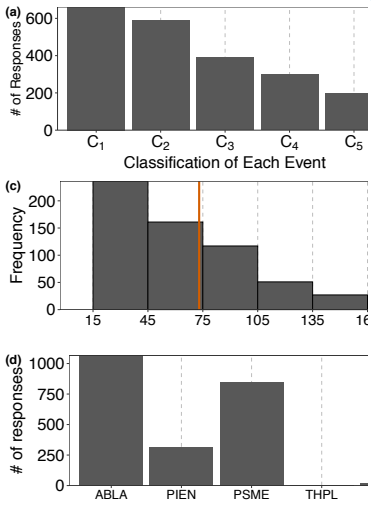

Deleted:

Deleted: ,

Deleted: percentage of classification of responses, (c)

Deleted: d

Deleted: obtained

Deleted: 66

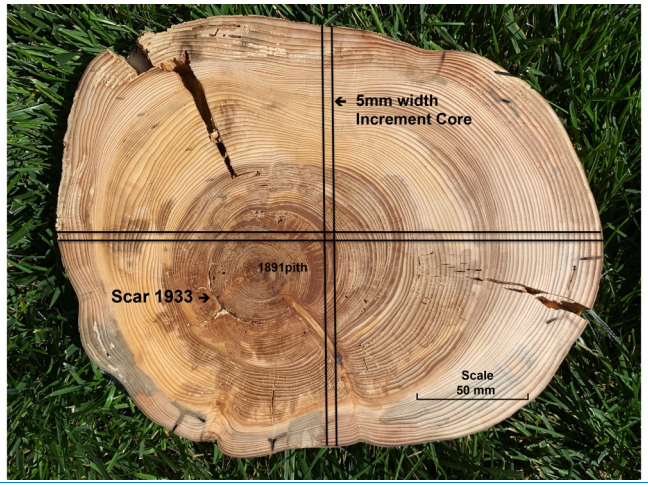

Figure 4: Example of cross section sample where 4 cores taken on uphill, downhill, and perpendicular (2) would have missed at least one scar (1933) and potentially the pith of the tree. The black lines indicate the potential cores using a 5 mm width increment borer.

3.2 Individual Path Chronologies

There were 49 avalanche events identified from GD responses across all 12 individual paths in the study region. The avalanche years most common throughout all of the individual path chronologies were: 2014 (7 paths); 1982 and 1990 (5 paths); and 1933, 1950, 1972, and 1974 (4 paths) (Figure 5 and Table 3). We identified the year with the greatest number of individual GD responses (2002) in 3 paths - two from JFS sub-region and one in the WF sub-region. There was no clear pattern showing paths physically closer in proximity to each other having more similarly identified avalanche years. However, paths within the WF sub-region produced the most similar number of large magnitude avalanche years. When we applied the W_{it} process step to more heavily weight higher quality signals, the number of identified avalanche years did not change for any individual avalanche path compared to application of the double threshold method alone. This highlights the number of responses classified as C_1 and C_2 (high quality) in our dataset.

Deleted:

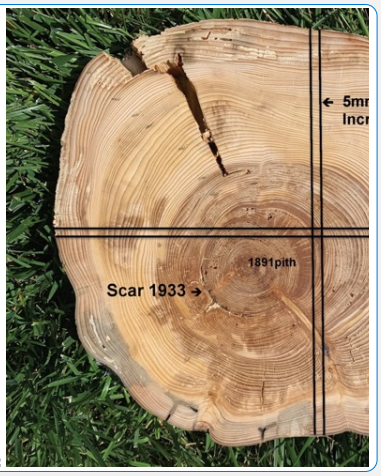

Deleted: .

Deleted: 4

Deleted: tree

Deleted: . Two of these paths were in the

Deleted: as well as the RMA path

Deleted: of

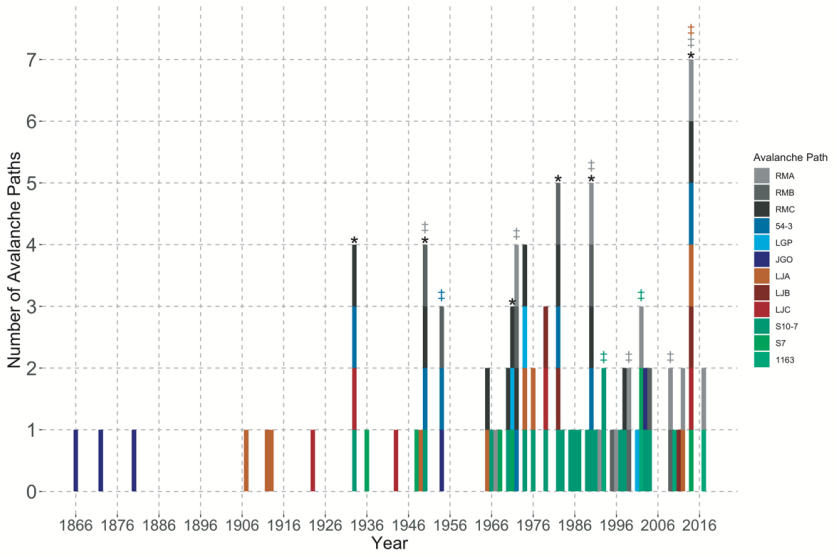

Figure 5: Number of individual avalanche paths in which an avalanche event occurred in any given year. Avalanche years with ‡ (gray=WF, dark blue = GTSR, orange = Swan, green= JFS) indicate years identified in at least two avalanche paths in the sub-region. * represents avalanche years in common in at least 1 path from at least three of the four sub-regions.

Deleted: identified per year.

Table 3: Avalanche chronologies and return interval (RI) statistics of all 12 avalanche paths in the region. Avalanche years in bold indicate years identified in at least two avalanche paths in the sub-region. Underlined avalanche years indicate years in common in at least 1 path from at least three of the four sub-regions. 1/RI refers to the probability of an avalanche occurring in that avalanche path in any given year. σ refers to the standard deviation of the RI. The period of record (POR) for each path represents earliest inner year to the most recent outer year of all raw samples in the path. The RI was calculated on the return interval of avalanche years.

	RMA	RMB	RMC	54-3	LGP	JGO	LJA	LJB	LJC	Shed 10-7	Shed 7	1163
Aval Years	1967 **1972** **1990** 1992 1996 **1999** 2002 **2009** 2012 **2014** 2017	**1950** 1954 **1972** 1982 **1990** 1995 **1999** 2004 **2009**	1933 **1950** 1965 1970 1971 **1972** 1974 1982 **1990** 1998 **2014**	1933 1950 **1954** 1972 1982 1990 2014	1971 2001 2009	1866 1872 1880 **1954** 2003	1907 1912 1913 1949 1965 1974 1976 2012 **2014**	1979 1982 2011 **2014**	1923 1933 1943 1979 **2014**	1933 1950 1966 1970 1974 1976 1979 1982 1983 1985 1986 1987 1989 1990 1991 **1993** 1997 1998 2003 2004	1936 1948 1968 1971 **2002** 2014	**1993** **2002** 2010 2017
# of aval. years	11	9	11	7	4	5	9	4	5	20	6	4
POR (raw samples)	1922-2017	1845-2017	1783-2016	1777-2017	1836-2009	1784-2017	1636-2017	1808-2017	1657-2017	1910-2004	1864-2017	1929-2017
RI - median	3	5	8	14	8	28.5	7	3	22.5	2	12	8
RI - mean	5	7.38	8.1	13.5	12.67	34.25	13.38	11.67	22.75	3.74	15.6	8
RI – min.	2	4	1	4	3	6	1	3	10	1	3	7
RI – max.	18	18	17	24	27	74	36	29	36	17	31	9
1/RI	0.33	0.20	0.13	0.07	0.13	0.13	0.14	0.33	0.04	0.50	0.08	0.13
σ	4.81	4.78	6.12	7.42	12.66	33.09	14.79	15.01	14.73	4.68	10.50	1.00

Across all individual paths, the median estimated return interval was 8 years with a range of 2 to 28.5 (Figure 6). JGO, located in the GTSR sub-region, exhibited the greatest spread in estimated return intervals followed by LJB. Hereafter, return intervals indicate median return intervals unless specified. The avalanche paths within the GTSR sub-region had the most similar return intervals of any of the sub-regions whereas the paths in the JFS sub-region exhibited substantial variability in median return interval values. The return interval

for JGO differed significantly from several other paths: RMA, RMB, RMC, and Shed 10-7 ($p \leq 0.01$). However, when we relax a strict cutoff of $p = 0.05$, the return interval from JGO also differed from 1163 ($p = 0.07$) and LJA ($p = 0.08$). Similarly, the return interval for Shed 10-7 differs from LJC ($p = 0.07$). In assessing the potential geomorphic controls on return interval, path length was the only significantly correlated characteristic ($r = 0.65$, $p = 0.02$, Figure A1).

We subset the period of record for each path from 1967-2017 and compared RI values to the full record. Nine paths exhibit no change in RI values when compared to the full record. In one path, 54-3, RI values decreased from 14 to 10 years. We observed larger changes in the other two paths; JGO path where only one avalanche year was recorded (down from 5 years) and the median RI in LJC changed from 22.5 years to 35 years.

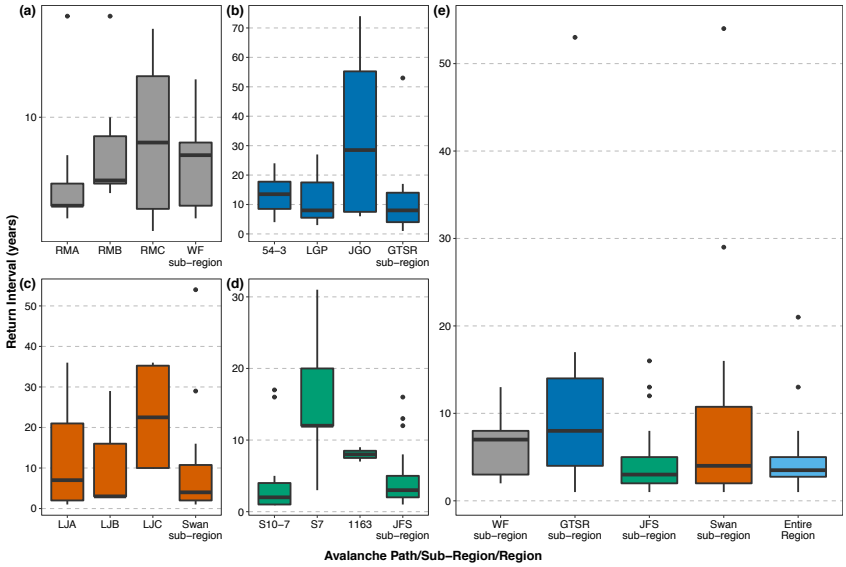

Figure 6: Boxplot of return intervals for individual avalanche paths in each sub-region: (a) WF, (b) GTSR, (c) Swan, and (d) JFS. (e) shows the median return intervals for the sub-regions and the overall region.

3.2 Sub-region Chronologies

When the paths were aggregated into sub-regions (three paths per sub-region) the median return periods for each sub-region were similar and all less than 10 years (Figure 6(e) and Table 4). The number of avalanche years for all of the sub-regions ranges from 12-18 with the greatest number of identified years in the JFS sub-region and the fewest in the WF sub-region. The JFS sub-region has the shortest median return interval followed by the Swan, WF, and GTSR sub-regions. The number of avalanche years for each aggregated sub-region is greater than the number of avalanche years for any individual path within each sub-region except

Deleted: 5

for the JFS sub-region where 18 avalanche years were identified but Shed 10-7 totaled 20 avalanche years (Table 5).

Deleted: 6

Table 4: Avalanche chronologies and return interval (RI) statistics of all four sub-regions. 1/RI refers to the probability of an avalanche occurring in that avalanche path in any given year. 1/RI refers to the probability of an avalanche occurring in that avalanche path in any given year. σ refers to the standard deviation of the RI.

	WF	GTSR	Swan	JFS	Region
# of aval. years	12	14	13	18	30
RI – median	7	8	4	3	3
RI – mean	6.27	11.35	11.25	4.94	5.21
RI – min.	2	1	1	1	1
RI – max.	13	53	54	16	53
1/RI	0.14	0.13	0.25	0.33	0.33
σ	3.69	13.48	15.70	4.60	9.53

Table 5: Number of avalanche events for each subregion, the mean of three individual paths in each region, and the overall aggregated region.

# of avalanche events		
Sub-region	**3 individual paths**	**Aggregated sub-region**
WF	11,9,11	12
GTSR	7,3,5	14
Swan	9,4,5	13
JFS	20,6,4	18
Region	30	

In terms of commonality of years between the sub-regions, 1982 is the only year identified in all of the four sub-regions (Figure 7). Avalanche years commonly identified in three sub-regions are 1950, 1954, 1974 and 2014. The JFS sub-region identified the greatest number of years exclusive to that sub-region (10 years). The WF sub-region shared the greatest number of years with other regions (11 years) followed by JFS (9 years), GTSR (8 years), and the Swan (7 years). In the only available comparison against an incomplete and limited historical record, the individual reconstructed avalanche chronologies of paths in the JFS sub-region captured 10-50% of the recorded large magnitude events over years 1908 to 2017.

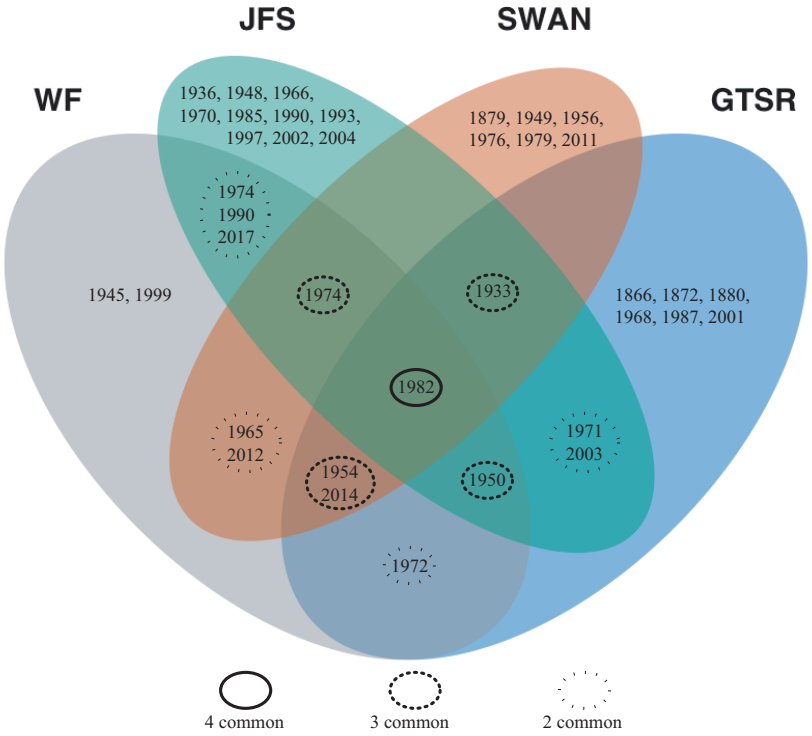

Figure 7: Venn diagram of avalanche years common between sub-regions. Overlapping areas of each ellipse indicate years in common with each sub-region.

3.3 Regional Chronology and RAAI

We identified 30 avalanche years in the overall region and a median return interval of 3 years (Table 5). The number of samples increases through time to a peak during 2005 and as expected the number of GD also increases through time (Figure 8(a)). The W_{it} index also increases, particularly from year 2000 onward with the largest spikes in 2014 and 2017 (Figure 8(b)). The regional assessment of avalanche years identified fewer years (n=30) than the simple aggregation of all unique avalanche years identified in the individual paths (n=49) (Table A2).

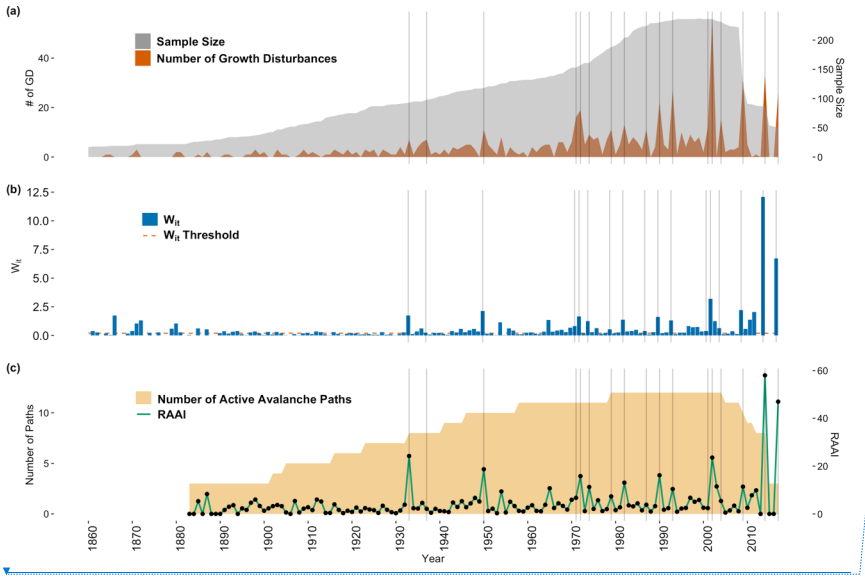

Deleted:

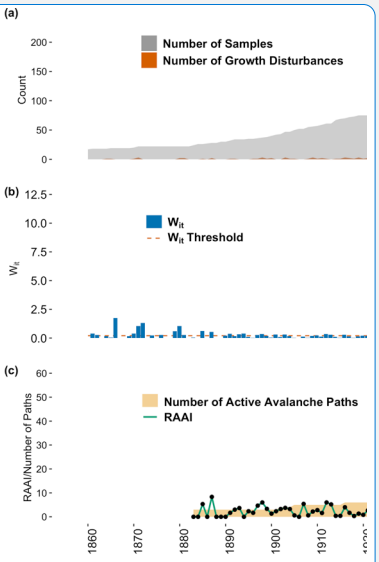

Figure 8: (a) The number of samples (gray shaded area) increases through time, but the number of responses (dark orange shaded area) varies. Note that sample size is on a secondary y-axis. (b) The W_{it} threshold (0.2, red dashed line) provides a means of discriminating between high and low confidence signals in the tree ring record. (c) The RAAI (green line, black points) is a measure of regional avalanche activity based on the I_t of each path and the number of active avalanche paths (yellow shaded area). Note RAAI is on a secondary y-axis.

When we included all paths but S10.7 (one of two paths with the greatest sample size), we captured 80% of all avalanche years and added one new year to the chronology (Table 7). When we removed LGP (the other path with the greatest sample size), we still captured all of the years in the regional chronology but introduced four new years into the chronology for a total of 34 years. A random sample of eight (two from each sub-region) of the 12 avalanche paths captured 83% of the years in the chronology and identified two new avalanche years. Finally, when using only one path from each sub-region with the largest samples size (Shed 10-7, 54-3, LJA, and RMA), we captured 73% of the avalanche years identified in the full regional chronology. When using a random sample of one path from each sub-region (1163, LGP, LJC, RMB), we captured only 43% of the years included in the regional chronology of all 12 paths. The RAAI is insensitive (no significant difference, $p > 0.05$) to the number of paths when tested using a minimum number of paths recording an avalanche in year *t*. The years with the largest RAAI are 2014 and 2017 followed by 2002, 1950 and 1933 (Figure 8(c)).

Table 6: Comparison of the number of avalanche years and RI when including all 12 paths in region to using a combination of fewer paths to define the region. HLC=high level of confidence and MLC=medium level of confidence as per Favillier et al. (2017,2018).

Paths	Region (All Paths)	All but S10.7	All but LGP	All but 54-3	S7, 1163, LGP, JGO, RMB, RMC, LJB, LJC	S10.7, 54-3, LJA, RMA	1163, LGP, LJC, RMB
# Paths	12	11	11	11	8	4	4
Sample Size (n)	635	528	526	581	382	253	239
# of Aval Years	30	27	34	31	27	34	17
# matches with regional	NA	24	30	29	25	22	13
# not in regional	NA	1	4	2	2	11	4
% captured in regional	NA	80	100	97	83	73	43
Median RI	3	3	3	3	3	2	3.5
# years removed using only W_{it} = HLC instead of W_{it} = MLC and HLC	10	3	9	7	1	1	1

To assess potential long-term trends in regional avalanche activity we implemented the modified Mann-Kendall test since the chronology exhibits weak serial autocorrelation. The full period of record of RAAI (1867-2017) exhibits a positive trend (tau = 0.186, Sens slope = -0.01, p = 0.006). The two other periods analyzed, 1950-2017 and 1990-2017, exhibit neither a positive nor a negative trend (p = *0*.36 and p = 0.95, respectively).

The probability of detection for the avalanche years (POD_{year}) identified in the regional chronology ranged from 8 to 58% when we examined individual paths (Table 7). The year with the highest *POD* was 2014. The mean *POD* for all years was 21%. When we examined avalanche paths that exhibited at least one scar during avalanche years identified in the regional chronologies, the *POD* is generally greater.

Deleted: 7

Deleted: 8

Table 7: Probability of Detection (POD_{year}). Avalanche years identified in the regional chronology and associated *POD* by analyzing individual paths with and without GD, sample size, and W_{it} thresholds.

Avalanche Year in Regional Chronology	POD (%) with thresholds	POD (%) without thresholds
1866	8	8
1872	8	8
1880	8	17
1933	33	58
1936	8	25
1945	NA	58
1948	8	33
1950	33	58
1954	25	67
1956	NA	58
1965	17	67
1970	17	50
1971	25	50
1972	33	83
1974	33	75
1976	17	50
1982	42	92
1990	42	83
1993	17	50
1997	8	92
1998	17	50
1999	17	58
2002	25	75
2003	17	33
2004	17	75
2009	17	33
2011	8	33
2012	17	42
2014	58	58
2017	17	25
Mean	**21**	**52**

Finally, the probability of capturing all of the avalanche years identified in the regional chronology by each individual path ranges from 7% to 40% (Table 8). The greatest POD_{path} value from any given path is S10.7 (*POD* = 40%) in the JFS sub-region followed by RMC in the Whitefish sub-region (*POD* = 37%). In general, the paths within the Whitefish sub-region capture the regional chronology most consistently.

Deleted: 8

Deleted: 9

Table 8: Probability of Detection of each individual path (POD_{path}) to the regional avalanche chronology.

Path	*POD* (%)
RMA	27
RMB	27
RMC	37
54-3	23
LGP	7
JGO	17
LJA	17
LJB	10
LJC	7
Shed 10-7	40
Shed 7	17
1163	10

4. Discussion

The processing and analysis of 673 samples spanning a large spatial extent allowed us to create a robust regional large magnitude avalanche chronology reconstructed using dendrochronological methods. Cross-sections provided a more robust and complete GD and avalanche chronology compared to a subsample generated from cores alone. Due to the reduced information value of working only with cores, Favillier et al. (2017) included a discriminatory step in their methods to distinguish avalanche signals in the tree-ring record from exogenous factors, such as abnormal climate signals or response to insect disturbance. By using cross sections to develop our avalanche chronologies, we were able to view the entire ring growth and potential disturbance around the circumference of the tree as opposed to the limited view provided by cores. This allowed us to place GD signals in context to both climate and insect disturbance without the need for this processing step.

We targeted sample collection in areas in the runout zones and along the trim line where large magnitude avalanches occurred in recent years. However, at several sites we also collected samples into the bottom of the track (S10.7, Shed 7, and 1163) rather than just the runout zone. Thus, some additional noise in the final chronology for those specific paths could be due to more frequent small magnitude avalanches. Though the oldest individual trees extended as far back as the mid-17th century, the application of the double thresholds and W_{it} processing steps restricted individual path avalanche chronology lengths since the minimum GD threshold requirements were not met. It is difficult to place much confidence in these older recorded events due to the decreasing evidence back in time inherent in avalanche path tree-ring studies. Therefore, we chose to examine more recent time periods dictated by the avalanche years identified through the double threshold methods.

All of the paths in the study are capable of producing large magnitude avalanches with path lengths greater than 100 m (typical length for avalanche destructive size 2, D2), and all but RMC have a typical path length of close to or greater than 1000 m (for avalanche destructive size 3, D3) (Greene et al., 2016) . As Corona et

Deleted: 9

Deleted: We identified 2134 GD from our samples, which is similar to Martin and Germain's (2016) study where they collected 458 cross sections and 350 cores, and reported 2251 GD.

Deleted: up

Deleted:).

Deleted: with a larger sample size and more consistent number of sites and individual series when considering return intervals and RAAI…

al. (2012) note, the avalanche event must be large enough to create an impact on the tree, and size D2 or greater will be evident from the tree-ring record (Reardon et al., 2008). However, the successive damage and removal of trees from events size D2 or greater also impacts the future potential to record subsequent events of similar magnitude. In other words, if a large magnitude avalanche removes a large swath of trees in one year, then there are fewer trees available to record a slightly smaller magnitude avalanche in subsequent years. Therefore, dendrochronology methods inherently underestimate avalanche events by up to 60% (Corona et al., 2012), and our results suggest these methods captured about 10-50% of the available historical record for JFS canyon.

4.1 Regional Sampling Strategy

By examining three different spatial scales (individual path, sub-region, and region) we produced a large magnitude avalanche chronology for the region captured in a small subset of the total number of paths across the large region. Accordingly, this sampling strategy may also alleviate the issue of recording large magnitude avalanches within a region in the successive years following a major destructive avalanche event that removed large number of trees within specific paths but not others. Overall, a regional sampling strategy enables us to capture large magnitude avalanche events over a broad spatial extent that is useful for regional avalanche forecasting operations and future climate association analysis. This strategy also allows us to understand large magnitude avalanche activity at scales smaller than the regional scale.

4.2 Chronologies for Individual Paths and Sub-Regions

We applied the W_{it} threshold specifically to weight higher quality signals. The number of identified avalanche years does not change for any individual avalanche path when we applied the W_{it} process. This suggests that many of the signals in our samples were ranked as high-quality (i.e. C_1-C_2). This can be attributed to the use of cross sections which allowed for a more complete depiction and assessment of the tree-ring signal (Carrara, 1979).

We developed avalanche chronologies for 12 individual avalanche paths. The path with the greatest number of identified avalanche years, S10.7, contains two major starting zones that are both steeper (35 and 39 degrees) than Shed 7, which also contains two separate starting zones. Reardon et al. (2008) collected a substantial number of samples at higher elevations in the S10.7 avalanche path. However, the location data for these samples were not available. Many of those samples were the living stumps that captured smaller annual events. This is likely the root of the difference for S10.7 and the reason this path contains the largest numbers of avalanche years in this analysis.

The range of return intervals across all paths (2 – 22.5 years) is similar to those reported for 12 avalanche paths across a smaller spatial extent in the Chic Choc Mountains of Quebec, Canada (2 – 22.8) (Germain et al., 2009). Although the authors in that study used a different avalanche signal index, this still suggests considerable variation in avalanche frequency across avalanche paths within a region.

Deleted: S10.7

JGO contains the maximum return interval for any path in the study, and the return intervals are significantly different than numerous other paths. A lack of recording data after one large avalanche event could easily skew this value. To understand if this value is accurate, we would have to sample adjacent tracks to determine if the return intervals are similar or not. Therefore, we cannot fully explain the large maximum return interval for this path. However, one potential explanation is that this path is the only one located east of the Continental Divide where the snowpack is often much shallower, particularly at lower elevations (Selkowitz et al., 2002), thus inhibiting frequent large magnitude events from impacting the sampled runout zone. The fetch upwind of this avalanche path is characterized by steep, rocky terrain harboring scoured slopes. This limits the amount of snow available for transport to the JGO starting zone which may also influence the load and stress placed upon this starting zone and subsequent large magnitude avalanches.

The greatest number of identified avalanche years is in the JFS sub-region. The avalanche paths in this sub-region are all south or southeasterly facing whereas the other sub-regions span a greater range of aspects. This may cause a bias toward a more unified representation of that aspect compared to the inclusion of other aspects in the JFS sub-region.

The return intervals for LJC in the Swan sub-region were the greatest in this sub-region and this is likely due to wildfire activity in this path in 2003. LJC was heavily burned, and this created a steep slope with few trees that was once moderately to heavily forested. Substantial anchoring and snowfall interception likely created an avalanche path without many large magnitude avalanches for decades since slope forestation plays a substantial role in runout distance and avalanche frequency in forested areas (Teich et al., 2012). In addition, wildfires in 1910 burned a majority of the JFS sub-region as well and the higher frequency of avalanche years recorded between 1910 and 1940 in S10.7 suggests this may also be a contributor to the high frequency of avalanche events in that location (Reardon et al., 2008). In addition, the fire in LJC may also have removed evidence of previous avalanche activity.

Our results also suggest that return interval increases as path length increases, though the sample size for this correlation analysis on individual paths is small (n=12). This is likely because only large magnitude avalanches affect the far extent of the runout of the path. This differs from a group of avalanche paths in Rogers Pass, British Columbia, Canada, where path length was not significantly correlated with avalanche frequency (Smith and McClung, 1997). However, that study used all observed avalanches, including artillery-initiated avalanches, as opposed to a tree-ring reconstructed dataset.

The differences between individual avalanche paths as well as sub-regions are likely due to localized terrain and weather/climate factors and the interaction of the two (Chesley-Preston, 2010). For example, Birkeland (2001) demonstrated significant variability of slope stability across a small mountain range dependent upon terrain and weather. Slope stability and subsequent large magnitude avalanching are likely to be highly heterogeneous across not only the sub-region, but across a large region. This is also consistent with findings by Schweizer et al. (2003) that suggest substantial differences in stability between sub-regions despite the presence of widespread weak layers. Finally, climate drives weather, but is not a first order effect on

Deleted: JGO contains the maximum return interval for any path in the study, and the return intervals are significantly different than numerous other paths. A lack of recording data after one large avalanche event could easily skew this value. Another potential explanation is that this path is the only one located east of the Continental Divide where the snowpack is often much shallower, particularly at lower elevations (Selkowitz et al., 2002), thus inhibiting frequent large magnitude events from impacting the sampled runout zone. The fetch upwind of this avalanche path is characterized by steep, rocky terrain harboring scoured slopes. This limits the amount of snow available for transport to the JGO starting zone which may also influence the load and stress placed upon this starting zone and subsequent large magnitude avalanches.¶
The greatest number of identified avalanche years is in the JFS sub-region. The avalanche paths in this sub-region are all south or southeasterly facing whereas the other sub-regions span a greater range of aspects. This may cause a bias toward a more unified representation of that aspect compared to the inclusion of other aspects in the JFS sub-region. ¶

avalanche occurrence in any one given avalanche path. In this study, we derived a regional avalanche chronology to provide a spatial scale that aligns more with the spatial scale of climate drivers than any one individual path. These are relationships that should be examined in future work.

4.3 Regional Chronologies and RAAI

The regional chronology we developed through the use of tree-ring analysis on collections made across 12 avalanche paths suggests, unsurprisingly, that the inclusion of more avalanche paths across a large spatial extent produces a more robust identification of major avalanche winters. When we aggregate all 12 paths together and apply established thresholds to discriminate the signal from the noise, we identified 30 avalanche years throughout the region. This allows us to place each year in context of the region, or full extent of the scale triplet, rather than simply collating all of the major avalanche winters identified in each individual path or sub-region. However, we also account for the support and spacing by including adjacent avalanche paths within a sub-region and multiple sub-regions throughout the region. This sampling strategy combined with the large sample size collected throughout the region allowed for a robust assessment of regional avalanche chronology derived from tree-ring records.

We tested the sensitivity of the term regional by removing specific and random paths. Our results suggest that removing paths from this structure, and subsequently compromising the sampling strategy, introduces noise. By reducing the sample size, we reduce the ability of the thresholds to filter out noise, thereby increasing the actual number of avalanche years in the region. However, the sample size reduction also reduces the number of identified avalanche winters common to the full 12 path regional record (Table 6). Our results emphasize the importance of sampling more paths spread throughout the region of interest as well as a large dataset across the spatial extent.

Avalanche path selection is clearly important when trying to assess avalanche frequency (de Bouchard d'Aubeterre et al., 2019), and this is supported by our results suggesting that S10.7 is more influential than any other path in our study (Table 6). This is also illustrated by the large number of avalanche years detected in S10.7 due to increased sampling in the track. However, selecting multiple paths throughout the region representing a wide range of geomorphic characteristics and potentially influenced by local weather patterns provides a reasonable assessment of regional avalanche activity in areas without historical records. By quantifying the sensitivity of the number of avalanche paths within a given region, we illustrate that sampling a greater number of avalanche paths dramatically increases the probability of identifying more avalanche years as well as increases the ability to reconstruct major avalanche cycle (widespread avalanche event) chronologies. However, as previously noted, dendrochronological techniques tend to underestimate avalanche frequency, which implies that caution should be used when interpreting a regional avalanche signal using this technique, particularly as sample numbers and qualities (e.g. cores vs. cross sections) decline.

Interestingly, the difference in median return interval throughout the "region" using 12 paths compared to using four or eight paths changes only slightly. This suggests that fewer paths are still able to represent the

Deleted: 7

Deleted: 7).

major avalanche return intervals across a region. However, choosing fewer paths appears to introduce more noise and therefore fewer years identified than a regional chronology with more avalanche paths.

The RAAI provides a measure of avalanche activity scaled to the number of active avalanche paths across the region through time. The years with the greatest RAAI value coincide with substantial activity provided in the historical record as well as previous dendrochronological studies from the JFS sub-region (Butler and Malanson, 1985a, b; Reardon et al., 2008). The winter of 1932-33 was characterized by heavy snowfall and persistent cold temperatures leading to extensive avalanche activity that destroyed roadway infrastructure in the JFS sub-region, 1950 saw a nearly month-long closure of U.S. Highway 2 due to avalanche activity, and in 2002, an avalanche caused a train derailment. While these are all confined to the JFS sub-region, with the exception of 2002, they are also years shared by at least two other sub-regions.

We examined the probability of detecting an avalanche year throughout the region by sampling any one given path. In seven of 30 years, the POD_{year} is only 8% and in all but three years the POD_{year} is less than 40%. The low *POD* values are distributed throughout the time series, suggesting decreasing sample size back in time or the number of active avalanche paths is not an influential factor. The POD is likely reflective of the spatial variability of large magnitude avalanche occurrence across a region. It also aligns with the observational findings of Mears (1992). During a major storm in 1986 throughout much of the western United States that deposited 30-60 cm of snow water equivalent, Mears (1992) reports that in the area around Gothic, Colorado less than 40% of avalanche paths produced avalanches and less than 10% produced avalanches approaching the 100-year return interval. This also confirms the wide variability of avalanche years between sub-regions recorded in our tree-ring record. Additionally, some of the avalanches in a given cycle may not be large enough to be reflected in the tree ring record. Therefore, low values of POD_{path} when considering only one avalanche path and identifying only one common year of large magnitude avalanche activity (1982) amongst the sub-regions through dendrochronology is not surprising. Paths with at least one GD (i.e. without applying thresholds) during avalanche years identified in the regional chronology exhibit a greater POD_{path}, but this greater POD_{path} comes at the expense of introducing more noise if we were to simply use one scar per path to define an avalanche event.

Deleted: scar

Our results also suggest that our sampling design using scale triplet increases the probability of detecting avalanche activity across an entire region. We note that we are only able to scale our probability calculations to our dataset with a limited historical observational record. However, our results illustrate the importance of sampling more paths if the goal is to reconstruct a regional chronology. In our dataset, the greatest value of POD_{path} is 40% suggesting that if by chance, we sampled this path we would have captured the regional avalanche activity 40% of the time.

The trends in RAAI over the entire period of record are likely influenced by the decreasing number of samples available to record an event further back in time. Despite the RAAI accounting for the number of avalanche paths (minimum of n = 3), the small sample size from the late 19th century precludes us from suggesting there

is a true increase in regional avalanche activity from 1867 to 2017. This is also supported by the absence of positive or negative trend from 1950 to 2017 and 1990 to 2017.

4.4 Limitations

Overall, our results strongly suggest that sampling one path, or multiple paths in one sub-region, is insufficient to extrapolate avalanche activity beyond those paths. Multiple paths nested within sub-regions are necessary to glean information regarding avalanche activity throughout those sub-regions as well as the overall region. Our study is still limited by the underrepresentation inherent in dendrochronological techniques for identifying all avalanche events. While we analyzed 673 samples over the extent of the region, some of the paths in our study had relatively small sample sizes per individual path as compared to recent suggestions (Corona et al., 2012). This may have influenced the number of avalanche years identified and subsequent return intervals per individual path. However, we attempted to limit the influence of sample size by using full cross-sections from trees, robust and critical identification of signals in the tree-rings, and appropriate established threshold techniques.

We also recognize that sampling more avalanche paths in our region would certainly provide a more robust regional avalanche chronology, but time, cost, and resource constraints required an optimized strategy. Finally, our study would undoubtedly have benefited from a longer and more accurate historical record for comparisons and verification of the tree-ring record in all of the sub-regions. Overall, our study illustrates the importance of considering spatial scale and extent when designing, and making inferences from, regional avalanche studies using tree-ring records.

5. Conclusions

We developed a large magnitude avalanche chronology using dendrochronological techniques for a region in the northern U.S. Rocky Mountains. Implementing a strategic sampling design allowed us to examine avalanche activity through time in single avalanche paths, four sub-regions, and throughout the region. By analyzing 673 samples from 12 avalanche paths, we identified 30 years with large magnitude events across the region and a median return interval of ~3 years (from 1866-2017). Large magnitude avalanche return interval and number of avalanche years vary throughout the sub-regions, suggesting the importance of local terrain and weather factors. Our work emphasizes the importance of sample size, scale, and spatial extent when attempting to derive a regional large magnitude avalanche chronology from tree-ring records. In our dataset, the greatest value of POD_{path} is 40% suggesting that if we sampled only this path, we would have captured the regional avalanche activity 40% of the time. This clearly demonstrates that a single path cannot provide a reliable regional avalanche chronology. Specifically, our results emphasize the importance of 1) sampling more paths spread throughout the region of interest; 2) collecting a large number of cross-sections relative to cores; and, 3) generating a large dataset that scales to the appropriate spatial extent. Future work

Deleted: .

should include conducting a similar study with a number of paths in the same sub-regions for verification, or in an area with a more robust regional historical record for verification.

6. Appendix A

Table A1: List of previous avalanche-dendrochronological work *with more than one avalanche path* in study – to place our regional work in context with other regional/multiple path studies. Number of samples, paths, growth disturbances (GD), and spatial extent (linear distance between most distant avalanche paths in study area) are included. For spatial extent, *NA* is reported in studies where spatial extent is not reported or could not be inferred from maps in the published work. Where spatial extent is not reported directly in previous work, it is estimated by using maps from the published work and satellite imagery. We included only the initial studies using a dataset with more than one avalanche path. For example, if a study used the same dataset again in subsequent work, we did not include it.

Authors	Location	# Trees	# Samples	# Paths	Spatial Extent	# GD
Gratton et al. (2019)	Northern Gaspé Peninsula, Québec, Canada	82	177 cores 65 x- sec	5	~20 km	Not provided
Meseşan et al. (2018)	Parâng Mountains, Carpathians, Romania	232	430 cores 39 x-sec 4 wedges	3	~16 km	Not provided
Favillier et al. (2018)	Zermatt valley, Switzerland	307	620 cores 60 x-sec	3	~1 km	2570
Ballesteros-Canovas (2018)	Kullu district, Himachal Pradesh, India	114	Not Provided	1 slope (multiple paths)	~ 1 km	521
Pop et al.(2018)	Piatra Craiului Mountains, Romania	235	402 cores 34 x-sec	2	~ 2 km	789
Martin and Germain (2016)	White Mountains, New Hampshire	450	350 cores 456 x-sec	7	~10 km	2251
Voiculescu et al. (2016)	Făgăras massif, Carpathians, Romania	293	586 cores	4	*NA*	853
Schläppy et al. (2015)	French Alps, France	967	1643 cores 333 x-sec	5	~100 km	3111
Schläppy et al. (2014)	French Alps, France	297	375 cores 63 x-sec	2	~100 km	713
Schläppy et al. (2013)	French Alps, France	587	1169 cores 122 x-sec	3	~100 km	1742
Casteller et al. (2011)	Santa Cruz, Argentina	95	~95 x-sec	9	~2 km	Not provided

Deleted: Table A1

Moved (insertion) [1]

Moved (insertion) [2]

Field Code Changed

Field Code Changed

Field Code Changed

Field Code Changed

Field Code Changed

Köse et al. (2010)	Katsomonu, Turkey	61	Not provided	2	~ 500 m	Not provided
Muntán et al. (2009)	Pyrenees, Catalonia	NA	448	6	~150 km	Not provided
Germain et al. (2009)	Northern Gaspé Peninsula, Québec, Canada	689	1214 x-sec	12	~30 km	2540
Butler and Sawyer (2008)	Lewis Range, Glacier National Park, Montana, USA	22	22 x-sec	2	~5 km	Not provided
Casteller et al. (2007)	Grisons, Switzerland	145	122 x-sec 52 cores 10 wedges	2	~ 20 km	Not provided
Germain et al. (2005)	Northern Gaspé Peninsula, Québec, Canada	142	142 x-sec	5	*NA*	420
Dube et al.(2004)	Northern Gaspé Peninsula, Québec, Canada	110	170 x-sec	3	~9 km	Not provided
Hebertson and Jenkins (2003)	Wasatch Plateau, Utah, USA	261	Not provided	16	*NA*	Not provided
Rayback (1998)	Front Range, Colorado, USA	98	58 trees cored (2-5 cores /tree) 31 x-sec 9 wedges	2	~7 km	Not provided
Bryant et al. (1989)	Huerfano Valley, Colorado, USA	180	Not provided	3	~2 km	Not provided
Butler and Malanson (1985a)	Lewis Range, Glacier National Park, Montana, USA	78	Not provided	2	~6 km	Not provided
Butler (1979)~	Glacier National Park, Montana, USA	NA	36 x-sec 17 cores	12	~15 km	Not provided
Smith (1973)	North Cascades, Washington, USA	NA	Not provided	11	~ 35 km	Not provided
Potter (1969)	Absaroka Mountains, Wyoming, USA	50	Not provided	5	~ 2 km	50

Table A2: Regional chronologies from the International Tree-Ring Database used for cross-dating.

MT Avalanche Project Site	ITRDB Tree-Ring Chron.	Originator	Date Range	Species	Coordinates	Elevation	NOAA data set ID
Going-to-the-Sun Road sites	Going to the Sun Road (GTS)	Gregory T. Pederson Jeremy S. Littell	1337 - 2002	PSME	48.42 -113.5167	1860M	noaa-tree-27540_MT159
John F. Stevens Canyon sites	Doody Mountain (DOO)	Gregory T. Pederson Blase Reardon	1660 - 2001	PSME	48.3833 -113.6167	1890M	noaa-tree-27536_MT155
Lost Johnny Creek sites	Preston Park (PP)	Bekker, M.F.; Tikalsky, B.P.; Fagre, D.B.; Bills, S.D.	1766 - 2006	ABLA	48.43 -113.39	2150M	noaa-tree-5993_MT117
Red Meadow sites	Numa Ridge Falls (NRF)	Gregory T. Pederson Brian Peters	1645 - 2001	PSME	48.51 -114.12	1695M	noaa-tree-27550_MT168

Table A3: Avalanche Years identified in the regional analysis (Region, n=29) and avalanche years identified in one or more paths in the individual avalanche path analysis (Ind. Paths Unique Years, n=49). Years in bold indicate years in common between the two sets (n=27).

Region	Ind. Paths Unique Years
1866	**1866**
1872	**1872**
1880	**1880**
	1907
	1912
	1913
	1923
1933	**1933**
1936	**1936**
	1943
1945	
1948	**1948**
	1949
1950	**1950**
1954	**1954**
1956	

Deleted: A2

1965	**1965**
	1966
	1967
	1968
1970	**1970**
1971	**1971**
1972	**1972**
1974	**1974**
1976	**1976**
	1979
1982	**1982**
	1983
	1985
	1986
	1987
	1989
1990	**1990**
	1991
	1992
1993	**1993**
	1995
	1996
1997	**1997**
1998	**1998**
	1999
	2001
2002	**2002**
2003	**2003**
2004	**2004**
2009	**2009**
	2010
2011	**2011**
2012	**2012**
2014	**2014**
2017	**2017**

762

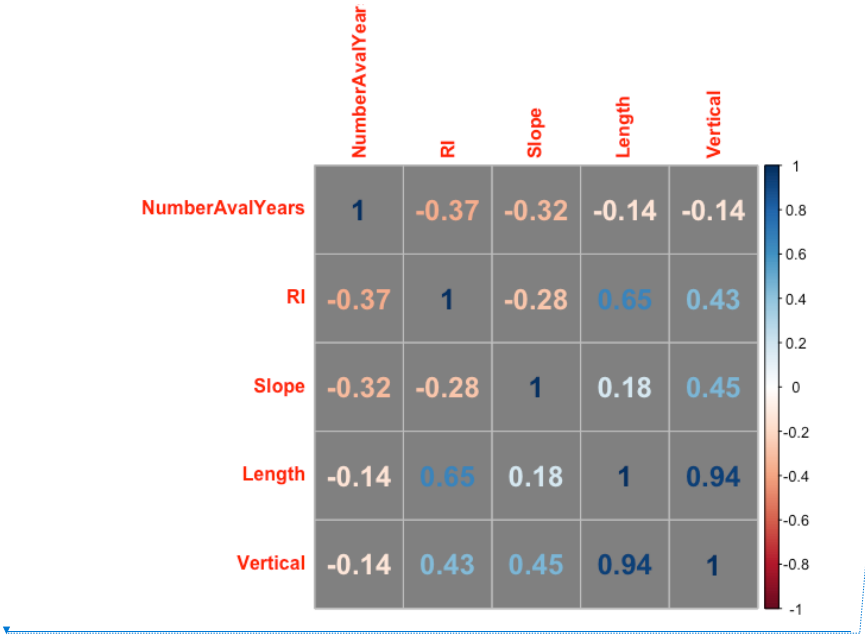

Figure A1: Correlation matrix (Pearson correlations coefficients) of the number of avalanche years, return interval (RI), starting zone slope angle (Slope), and path length (Length).

Deleted:

7. Data availability

Data for this work can be found in ScienceBase repository: Peitzsch, E. H., Stahle, D. K., Fagre, D. B., Clark, A. M., Pederson, G. T., Hendrikx, J., and Birkeland, K. W.: Tree ring dataset for a regional avalanche chronology in northwest Montana, 1636-2017. U.S. Geological Survey., U.S. Geological Survey data release, https://doi.org/10.5066/P9TLHZAI, 2019.

8. Author contribution

EP responsible for study conception and design, data collection, analysis, writing. JH contributed to development of study design, methods, editing, and writing. DS responsible for data collection, tree-ring processing and analysis and writing. GP, KB, and DF contributed to study design, editing and writing.

9. Disclaimer

Any use of trade, firm, or product names is for descriptive purposes only and does not imply endorsement by the U.S. Government.

10. Acknowledgements

We extend gratitude to Adam Clark for his substantial data collection efforts and Zach Miller for his assistance processing samples. This work was supported by the USGS Land Resources Western Mountain Initiative project.

11. References

Armstrong, B. R.: A quantitative analysis of avalanche hazard on U.S. Highway 550, southwestern Colorado, in: Proceedings of the Western Snow Conference, St. George, Utah, April 14-16, 2017, 95-104, 1981.

Ballesteros-Canovas, J. A., Trappmann, D., Madrigal-Gonzalez, J., Eckert, N., and Stoffel, M.: Climate warming enhances snow avalanche risk in the Western Himalayas, Proc. Natl. Acad. Sci. U.S.A., 115, 3410-3415, 10.1073/pnas.1716913115, 2018.

Bebi, P., Kulakowski, D., and Rixen, C.: Snow avalanche disturbances in forest ecosystems-State of research and implications for management, For. Ecol. and Manage., 257, 1883-1892, 10.1016/j.foreco.2009.01.050, 2009.

Birkeland, K. W.: Spatial patterns of snow stability throughout a small mountain range, J. Glaciol., 47, 176-186, 10.3189/172756501781832250 2001.

Blöschl, G., and Sivapalan, M.: Scale issues in hydrological modelling: A review, Hydrol. Processes, 9, 251-290, 10.1002/hyp.3360090305 1995.

Blöschl, G.: Scaling issues in snow hydrology, Hydrol. Processes, 13, 2149-2175, 10.1002/(SICI)1099-1085(199910)13:14/15%3C2149::AID-HYP847%3E3.0.CO;2-8, 1999.

Bryant, C.L., Butler, D.R., Vitek, J.D.: A statistical analysis of tree-ring dating in conjunction with snow avalanches – comparison of on-path versus off-path responses, Environ. Geol. Water Sci., 14, 53-59, 10.1007/BF01740585, 1989.

Burrows, C. J., and Burrows, V. L.: Procedures for the study of snow avalanche chronology using growth layers of woody plants, Institute of Arctic and Alpine Research, University of Colorado, Boulder, CO, Occasional Paper No. 23, 56 pp., 1976.

Butler, D. R.: Snow avalanche path terrain and vegetation, Glacier National Park, Montana, Arc. and Alp. Res., 11, 17-32, 10.1080/00040851.1979.12004114, 1979.

Butler, D. R., and Malanson, G., P.: A history of high-magnitude snow avalanches, southern Glacier National Park, Montana, U.S.A., Mt. Res. Dev., 5, 175-182, 10.2307/3673256, 1985a.

Butler, D. R., and Malanson, G. P.: A reconstruction of snow-avalanche characteristics in Montana, U.S.A., using vegetative indicators, J. of Glaciol., 31, 185-187, 10.3189/S0022143000006444, 1985b.

Butler, D. R., Malanson, G. P., and Oelfke, J. G.: Tree-ring analysis and natural hazard chronologies: minimum sample sizes and index values, Prof. Geogr., 39, 41-47, 10.1111/j.0033-0124.1987.00041.x, 1987.

Butler, D. R., and Sawyer, C. F.: Dendrogeomorphology and high-magnitude snow avalanches: a review and case study, Nat. Hazard Earth Sys., 8, 303-309, 10.5194/nhess-8-303-2008, 2008.

Colorado Avalanche Information Center Statistics and Reporting. http://avalanche.state.co.us/accidents/statistics-and-reporting/, last access: June 8, 2020.

Carrara, P. E.: The determination of snow avalanche frequency through tree-ring analysis and historical records, Geol. Soc. Am. Bull., 90, 773-780, 10.1130/0016-7606(1979)90%3C773:TDOSAF%3E2.0.CO;2, 1979.

Casteller, A., Stoeckli, V., Villalba, R., Mayer, A.C.: An evaluation of dendroecological indicators of snow avalanches in the Swiss Alps, Arct. Antarct. Alp. Res., 39, 218-228, 10.1657/1523-0430(2007)39[218:AEODIO]2.0.CO;2, 2007.

Casteller, A., Villalba, R., Araneo, D., and Stöckli, V.: Reconstructing temporal patterns of snow avalanches at Lago del Desierto,southern Patagonian Andes, Cold Reg. Sci. Technol., 67, 68-78, 10.1016/j.coldregions.2011.02.001, 2011.

Chesley-Preston, T.: Patterns of natural avalanche activity associated with new snow water equivalence and upper atmospheric wind direction and speed in the mountains surrounding Gothic, Colorado, Master of Science, Department of Earth Sciences, Montana State University, Bozeman, Montana, 75 pp., 2010.

Corona, C., Lopez Saez, J., Stoffel, M., Bonnefoy, M., Richard, D., Astrade, L., and Berger, F.: How much of the real avalanche activity can be captured with tree rings? An evaluation of classic dendrogeomorphic approaches and comparison with historical archives, Cold Reg. Sci. Technol., 74-75, 31-42, 10.1016/j.coldregions.2012.01.003, 2012.

de Bouchard d'Aubeterre, G., Favillier, A., Mainieri, R., Lopez Saez, J., Eckert, N., Saulnier, M., Peiry, J. L., Stoffel, M., and Corona, C.: Tree-ring reconstruction of snow avalanche activity: Does avalanche path selection matter?, Sci. Total Environ., 684, 496-508, 10.1016/j.scitotenv.2019.05.194, 2019.

Dube, S., Filion, L., and Hetu, B.: Tree-Ring Reconstruction of High-Magnitude Snow Avalanches in the Northern Gaspe Peninsula, Quebec, Canada, Arct. Antarct. Alp. Res., 36, 555-564, 10.1657/1523-0430(2004)036[0555:TROHSA]2.0.CO;2, 2004.

Favillier, A., Guillet, S., Morel, P., Corona, C., Lopez Saez, J., Eckert, N., Ballesteros Cánovas, J. A., Peiry, J.-L., and Stoffel, M.: Disentangling the impacts of exogenous disturbances on forest stands to assess multi-centennial tree-ring reconstructions of avalanche activity in the upper Goms Valley (Canton of Valais, Switzerland), Quat. Geochronol., 42, 89-104, 10.1016/j.quageo.2017.09.001, 2017.

Favillier, A., Guillet, S., Trappmann, D., Morel, P., Lopez-Saez, J., Eckert, N., Zenhäusern, G., Peiry, J.-L., Stoffel, M., and Corona, C.: Spatio-temporal maps of past avalanche events derived from tree-ring analysis: A case study in the Zermatt valley (Valais, Switzerland), Cold Reg. Sci. Technol., 154, 9-22, 10.1016/j.coldregions.2018.06.004, 2018.

Germain, D., Filion, L., and Hétu, B.: Snow avalanche activity after fire and logging disturbances, northern Gaspé Peninsula, Quebec, Canada, Can. J. of Earth Sci., 42, 2103-2116, 10.1139/e05-087, 2005.

Germain, D., Filion, L., and Hétu, B.: Snow avalanche regime and climatic conditions in the Chic-Choc Range, eastern Canada, Clim. Change, 92, 141-167, 10.1007/s10584-008-9439-4, 2009.

Germain, D., Hétu, B., and Filion, L.: Tree-ring based reconstruction of past snow avalanche events and risk assessment in Northern Gaspé Peninsula (Québec, Canada), in: Tree Rings and Natural Hazards - A State-

878 of-the-Art, edited by: Stoffel, M., Bollschweiler, M., Butler, D. R., and Luckman, B. H., Advances in Global
879 Change Research, Springer, London, 51-73, 2010.
880
881 Google. (n.d.). [Imagery of study area, northwest Montana]. Retrieved February 4, 2020 using R statistical
882 package get_map.
883
884 Gratton, M., Germain, D., and Boucher, É.: Meteorological triggering scenarios of tree-ring-based snow
885 avalanche occurrence on scree slopes in a maritime climate, Eastern Canada, Phys. Geogr., 1-18,
886 10.1080/02723646.2019.1573622, 2019.
887
888 Greene, E., Birkeland, K. W., Elder, K., McCammon, I., Staples, M., and Sharaf, D.: Snow, weather, and
889 avalanches: Observation guidelines for avalanche programs in the United States (3rd ed), American
890 Avalanche Association, Victor, ID, 104 pp., 2016.
891
892 Grissino-Mayer, H.: Evaluating crossdating accuracy: A manual and tutorial for the computer
893 program COFECHA, Tree-Ring Res., 57, 205-221, 2001.
894
895 Hamed, K. H., and Rao, A. R.: A modified Mann-Kendall trend test for autocorrelated data, J. Hydrol., 204,
896 182-196, 10.1016/S0022-1694(97)00125-X, 1998.
897
898 Hebertson, E. G., and Jenkins, M. J.: Historic climate factors associated with major avalanche years on the
899 Wasatch Plateau, Utah, Cold Reg. Sci. Technol., 37, 315-332, 10.1016/S0165-232x(03)00073-9, 2003.
900
901 Hendrikx, J., Murphy, M., and Onslow, T.: Classification trees as a tool for operational avalanche forecasting
902 on the Seward Highway, Alaska, Cold Reg. Sci. and Technol., 97, 113-120,
903 10.1016/j.coldregions.2013.08.009, 2014.
904
905 Holmes, R. L.: Analysis of tree rings and fire scars to establish fire history, Tree-Ring Bulletin, 43, 51-67,
906 1983.
907
908 International Tree Ring Data Bank (ITRDB): https://www.ncdc.noaa.gov/data-access/paleoclimatology-
909 data/datasets/tree-ring, access: March 1, 2018.
910
911 Kogelnig-Mayer, B., Stoffel, M., Schneuwly-Bollschweiler, M., Hübl, J., and Rudolf-Miklau, F.:
912 Possibilities and Limitations of Dendrogeomorphic Time-Series Reconstructions on Sites Influenced by

913 Debris Flows and Frequent Snow Avalanche Activity, Arct. Antarct. Alp. Res., 43, 649-658, 10.1657/1938-
914 4246-43.4.649, 2011.
915
916 Korpela, M., Wickham, H., Jackson, S. ggmap v3.0.0 – Spatial Visualization with ggplot2.
917 https://github.com/dkahle/ggmap. 2019.
918
919 Köse, N., Aydın, A., Akkemik, Ü., Yurtseven, H., and Güner, T.: Using tree-ring signals and numerical
920 model to identify the snow avalanche tracks in Kastamonu, Turkey, Nat. Hazards, 54, 435-449,
921 10.1007/s11069-009-9477-x, 2010.
922
923 Malevich, S. B., Guiterman, C. H., and Margolis, E. Q.: burnr : Fire history analysis and graphics in R,
924 Dendrochronologia, 49, 9-15, 10.1016/j.dendro.2018.02.005, 2018.
925
926 Mann, H. B.: Nonparametric tests against trend, Econometrica, 13, 245-259, 10.2307/1907187, 1945.
927
928 Martin, J. P., and Germain, D.: Dendrogeomorphic reconstruction of snow avalanche regime and triggering
929 weather conditions: A classification tree model approach, Prog. Phys. Geog., 10.1177/0309133315625863,
930 2016.
931
932 Mears, A. I.: Snow-Avalanche Hazard Analysis for Land-use Planning and Engineering, Colorado
933 Geological Survey Bulletin, 49, 55 pp., 1992.
934
935 Meseșan, F., Gavrilă, I. G., and Pop, O. T.: Calculating snow-avalanche return period from tree-ring data,
936 Nat. Hazards, 94, 1081-1098, 10.1007/s11069-018-3457-y, 2018.
937
938 Mock, C. J., and Birkeland, K. W.: Snow avalanche climatology of the western United States mountain
939 ranges, Bull. Am. Meteorol. Soc., 81, 2367-2392, 10.1175/1520-
940 0477(2000)081%3C2367:SACOTW%3E2.3.CO;2, 2000.
941
942 Mock, C. J., Carter, K. C., and Birkeland, K. W.: Some Perspectives on Avalanche Climatology, Ann. Am.
943 Assoc. of Geogr., 1-10, 10.1080/24694452.2016.1203285, 2016.
944
945 Muntan, E., Garcia, C., Oller, P., Marti, G., Garcia, A., and Gutierrez, E.: Reconstructing snow avalanches
946 in the Southeastern Pyrenees, Nat. Hazard Earth Sys., 9, 1599-1612, 10.5194/nhess-9-1599-2009, 2009.
947

948 Ott, R. L., and Longnecker, M. T.: An Introduction to Statistical Methods and Data Analysis, 7th Edition ed.,
949 Cengage Learning, Boston, MA, 1296 pp., 2016.
950
951 Peitzsch, E. H., Stahle, D. K., Fagre, D. B., Clark, A. M., Pederson, G. T., Hendrikx, J., and Birkeland, K.
952 W.: Tree ring dataset for a regional avalanche chronology in northwest Montana, 1636-2017. U.S. Geological
953 Survey., U.S. Geological Survey data release, 10.5066/P9TLHZAI, 2019.
954
955 Pop, O. T., Munteanu, A., Flaviu, M., Gavrilă, I.-G., Timofte, C., and Holobâcă, I.-H.: Tree-ring-based
956 reconstruction of high-magnitude snow avalanches in Piatra Craiului Mountains (Southern Carpathians,
957 Romania), Geografiska Annaler: Series A, Phys. Geogr., 100, 99-115, 10.1080/04353676.2017.1405715,
958 2018.
959
960 Potter, N.: Tree-ring dating of snow avalanche tracks and the geomorphic activity of avalanches, Northern
961 Absaroka Mountains, Wyoming, Geol. S. Am. S., Special Paper 123, 141-165, 1969.
962
963 Rayback, S. A.: A dendrogeomorphological analysis of snow avalanches in the Colorado Front Range, USA,
964 Phys. Geogr., 19, 502-515, 10.1080/02723646.1998.10642664, 1998.
965
966 Reardon, B. A., Pederson, G. T., Caruso, C. J., and Fagre, D. B.: Spatial reconstructions and comparisons of
967 historic snow avalanche frequency and extent using tree rings in Glacier National Park, Montana, U.S.A.,
968 Arct. Antarct. Alp. Res., 40, 148-160, 10.1657/1523-0430(06-069)[REARDON]2.0.CO;2, 2008.
969
970 Schläppy, R., Jomelli, V., Grancher, D., Stoffel, M., Corona, C., Brunstein, D., Eckert, N., and Deschatres,
971 M.: A New Tree-Ring-Based, Semi-Quantitative Approach for the Determination of Snow Avalanche
972 Events: use of Classification Trees for Validation, Arct. Antarct. Alp. Res., 45, 383-395, 10.1657/1938-4246-
973 45.3.383, 2013.
974
975 Schläppy, R., Eckert, N., Jomelli, V., Stoffel, M., Grancher, D., Brunstein, D., Naaim, M., and Deschatres,
976 M.: Validation of extreme snow avalanches and related return periods derived from a statistical-dynamical
977 model using tree-ring techniques, Cold Reg. Sci. Technol., 99, 12-26, 10.1016/j.coldregions.2013.12.001,
978 2014.
979
980 Schläppy, R., Jomelli, V., Eckert, N., Stoffel, M., Grancher, D., Brunstein, D., Corona, C., and Deschatres,
981 M.: Can we infer avalanche–climate relations using tree-ring data? Case studies in the French Alps, Reg.
982 Environ. Change, 16, 629-642, 10.1007/s10113-015-0823-0, 2015.
983

Schweizer, J.: Snow avalanche formation, Reviews of Geophysics, 41, 10.1029/2002rg000123, 2003.

Schweizer, J., Kronholm, K., and Wiesinger, T.: Verification of regional snowpack stability and avalanche danger, Cold Reg. Sci. and Technol., 37, 277-288, 10.1016/s0165-232x(03)00070-3, 2003.

Selkowitz, D. J., Fagre, D. B., and Reardon, B. A.: Interannual variations in snowpack in the Crown of the Continent Ecosystem, Hydrol. Process., 16, 3651-3665, 10.1002/hyp.1234, 2002.

Shroder, J. F.: Dendrogeomorphological analysis of mass movement on Table Cliffs Plateau, Utah, Quaternary Res., 9, 168-185, 10.1016/0033-5894(78)90065-0, 1978.

Šilhán, K., and Tichavský, R.: Snow avalanche and debris flow activity in the High Tatras Mountains: New data from using dendrogeomorphic survey, Cold Reg. Sci. Technol., 134, 45-53, 10.1016/j.coldregions.2016.12.002, 2017.

Skøien, J. O., and Blöschl, G.: Sampling scale effects in random fields and implications for environmental monitoring, Environ. Monit. Assess., 114, 521-552, 10.1007/s10661-006-4939-z, 2006.

Smith, L.: Indication of snow avalanche periodicity through interpretation of vegetation patterns in the North Cascades, Washington , in: Methods of Avalanche Control on Washington Mountain Highways: Third Annual Report, Washington State Highway Commission Department of Highways, Olympia, Washington, USA, 187 pp., 1973.

Smith, M. J., and McClung, D. M.: Avalanche frequency and terrain characteristics at Rogers' pass, British Columbia, Canada, J. Glaciol., 43, 165-171, 10.3189/S0022143000002926, 1997.

Stokes, M. A., and Smiley, T. L.: An Introduction to Tree-Ring Dating, The University of Arizona Press, Tucson, 1996.

Teich, M., Bartelt, P., Grêt-Regamey, A., and Bebi, P.: Snow Avalanches in Forested Terrain: Influence of Forest Parameters, Topography, and Avalanche Characteristics on Runout Distance, Arct. Antarct. Alp. Res., 44, 509-519, 10.1657/1938-4246-44.4.509, 2012.

Voiculescu, M., Onaca, A., and Chiroiu, P.: Dendrogeomorphic reconstruction of past snow avalanche events in Bâlea glacial valley–Făgăraş massif (Southern Carpathians), Romanian Carpathians, Quatern. Int., 415, 286-302, 10.1016/j.quaint.2015.11.115, 2016.

Deleted: ¶

Page 2: [1] Deleted Erich Peitzsch 11/2/20 10:51:00 AM